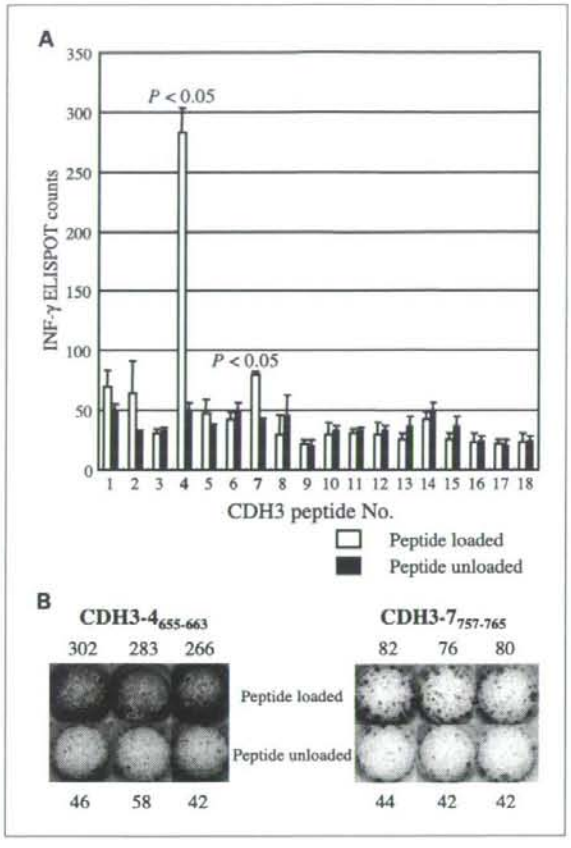

Fig. 3. Identification of HLA-A2–restricted mouse CTL epitopes of human CDH3 by using HLA-A2.1 (HHD) Tgm. *A*, we immunized the HLA-A2.1 (HHD) Tgm with 5×10^5 syngeneic BM-DCs pulsed with 18 candidate peptides *in vivo* at days 7 and 14. On day 21, $CD4^-$ spleen cells isolated from immunized mice were stimulated by BM-DCs pulsed with each peptide for 6 d. The CTL-producing IFN-γ was detected by an ELISPOT assay. We found that CDH3-$4_{655-663}$ (FILPVLGAV) and CDH3-$7_{757-765}$ (FIIENLKAA) were shown to induce peptide-reactive CTL. *B*, $CD4^-$ spleen cells showed 283.7 ± 40.0 spot counts per well, in response to the BM-DC pulsed with the CDH3-$4_{655-663}$ peptide (*top left*), whereas they showed 48.7 ± 11.9 spot counts per well in the presence of BM-DC without peptide loading (*bottom left*; $P < 0.05$). Similarly, $CD4^-$ spleen cells showed 79.3 ± 3.2 spot counts per well, in response to the BM-DC pulsed with the CDH3-$7_{757-765}$ peptide (*top right*), whereas they showed 42.7 ± 2.5 spot counts per well in the presence of BM-DC without peptide loading (*bottom right*; $P < 0.05$). These assays were done twice with similar results.

Subsequently, we asked whether these CTLs were able to kill human cancer cell lines expressing CDH3 and HLA-A2. As shown in Fig. 4B, the CDH3-reactive CTLs stimulated with CDH3-$4_{655-663}$ peptide exhibited cytotoxicity to HCT116 ($CDH3^+$, HLA-$A2^+$), HSC3 ($CDH3^+$, HLA-$A2^+$), and PANC1/CDH3 ($CDH3^+$, HLA-$A2^+$), PANC1 cells transfected with *CDH3* gene, but not to PANC1 ($CDH3^-$, HLA-$A2^+$), SKHep1 ($CDH3^-$, HLA-$A2^+$), and PK8 ($CDH3^+$, HLA-$A2^-$), in healthy donors. Similarly, the CTLs stimulated with CDH3-$7_{757-765}$ peptide exhibited cytotoxicity to HSC3, but not to PANC1, PK8, or SKHep1.

These cytotoxic activities were observed in the CTLs derived from various cancer patients (Fig. 4C). We used PANC1/CDH3 and SKHep1/CDH3 ($CDH3^+$, HLA-$A2^+$), SKHep1 cells transfected with the *CDH3* gene, as target cells to confirm that these peptides were processed naturally from the CDH3 protein in the cancer cells. As shown in Fig. 4C, the CTLs induced by stimulation with CDH3-$4_{655-663}$ or with CDH3-$7_{757-765}$ peptide revealed cytotoxicity against HCT116, PANC1/CDH3, and SKHep1/CDH3, but not to PANC1, SKHep1, or PK8. These results suggest that these peptides could be naturally processed and expressed on the surface of cancer cells in the context of HLA-A2 molecules. As a result, the CDH3-reactive CTLs had specific cytotoxicity to the cancer cells expressing both endogenous CDH3 and HLA-A2 molecules.

To confirm that the induced CTLs recognized the target cells in an HLA class I–restricted manner, we used the mAb against HLA class I (W6/32) to block the recognition by the CTLs. In this experiment, the anti–HLA class I antibody could markedly inhibit the IFN-γ production stimulated with SKHep1/CDH3 cells in an ELISPOT assay of the CTLs generated by stimulation with CDH3-$4_{655-663}$ peptide, with statistical significance (Fig. 4D, *left*; $P < 0.01$), and could inhibit the cytotoxicity of the CTLs against the HCT116 cells in a ^{51}Cr release assay (Fig. 4D, *middle*). Similarly, the anti–class I antibody could markedly inhibit the IFN-γ production stimulated with HSC3 cells in an ELISPOT assay of the CTLs generated by stimulation with CDH3-$7_{757-765}$ peptide (Fig. 4D, *right*; $P < 0.05$). These results clearly indicate that these induced CTLs recognized the target cells expressing CDH3 in an HLA class I–restricted manner.

In vivo *antitumor activity of adoptively transferred CDH3-induced human CTLs in NOD/SCID mice.* To assess the therapeutic efficacy of the CDH3-reactive CTL inoculation into the mice implanted with the $CDH3^+$ human cancer cell, we inoculated s.c. HCT116 positive for both CDH3 and HLA-A2 into NOD/SCID mice and injected i.v. human CTLs generated by stimulating the peripheral blood $CD8^+$ T cells with CDH3-$4_{655-663}$ and CDH3-$7_{757-765}$ peptides or control-irrelevant HIV peptide into mice when the diameter of these tumors reached 5 × 5 mm in size, as described in Materials and Methods. The control HIV peptide–stimulated $CD8^+$ T cells did not exhibit cytotoxicity against the HCT116 cells *in vitro* (data not shown). The tumor size of seven individual mice in each group (Fig. 5A) and the mean ± SD of the tumor sizes in each group (Fig. 5B) were evaluated. The control T-cell lines did not exhibit an inhibitory effect on the tumor growth, and PBS alone did not do so. The tumor size in the mice inoculated with the CDH3-stimulated CTLs was significantly smaller than those inoculated with the control HIV peptide–induced $CD8^+$ T cells or with PBS alone ($P < 0.001$). These results clearly indicate the efficacy of adoptive transfer therapy of CDH3-reactive human CTLs against $CDH3^+$ human tumor in NOD/SCID mice.

Discussion

In the current study, we identified a novel TAA, CDH3/P-cadherin, using a cDNA microarray analysis of pancreatic cancer. *CDH3* was strongly expressed in pancreatic cancer cells and faintly expressed in ovary and mammary gland based on the cDNA microarray analysis. The *CDH3* expression was barely detectable in other vital organs. Furthermore, our microarray and RT-PCR data showed that *CDH3* was expressed in gastric and colorectal cancers, as well as in pancreatic cancer, and not in their

normal counterparts. According to the findings of immunohistochemical analyses, CDH3 was overexpressed in the majority of pancreatic cancer cells, whereas the normal duct and the acinar cells in the pancreas showed a very weak expression at the protein level. These results suggest that targeting CDH3 could be a novel immunotherapeutic approach for these cancers, without the development of autoimmune diseases.

The cadherin family is divided into several subfamilies, including CDH1/E-cadherin, CDH2/N-cadherin, and CDH3/P-cadherin, designated by their tissue distribution. CDH1 is the predominant cadherin family member expressed in all epithelial tissues. It is well known that CDH1 is assumed to act as a tumor suppressor, negatively regulating the invasion and metastasis of tumor cells, in several malignancies (42–44). CDH2 is up-regulated in several invasive cancers and contributes to an invasive phenotype by interacting with fibroblast growth factor receptor and by downstream signaling (45). The expression and role of CDH3 in cancer are still poorly understood. In a previous study, Taniuchi et al. showed the up-regulation of CDH3 to be likely related to the biological aggressiveness of pancreatic cancer by interacting with p120ctn and activating Rho family GTPase, Rac1, and Cdc42 (46). Additional previous studies suggested the up-regulation of CDH3 to be a factor in the aggressive biological behavior and poor prognosis of both breast (26–28) and endometrial cancers (29). A recent report summarized that the objective response rate of cancer vaccine in clinical trials was low (2.6%; ref. 47). One possible reason is that the immune escape of cancer cells attributed to deletion, mutation, or down-regulation of the TAAs occurs as a consequence of therapeutically driven immune selection. Based from the standpoint that tumor cells cannot lose antigens which are required for tumorigenesis, we considered CDH3 as a candidate TAA useful for anticancer immunotherapy.

In this study, we identified two HLA-A2–restricted CDH3 epitope peptides, which could stimulate the generation of

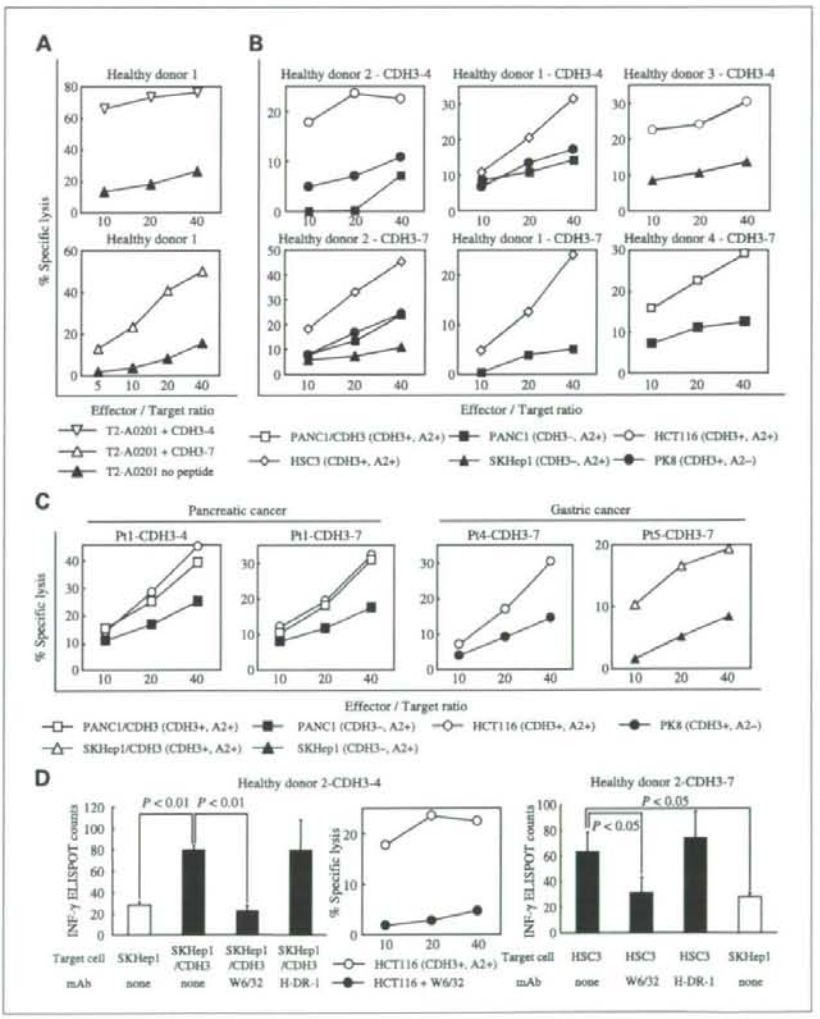

Fig. 4. Induction of CDH3-specific human CTL from the PBMCs of HLA-A2– positive healthy donors and cancer patients. *A*, the CDH3 peptide-reactive CTLs were generated from the PBMCs of HLA-A2– positive healthy donors. After three stimulations with autologous monocyte-derived DCs pulsed with the CDH3-$4_{655-663}$ (*top*) or CDH3-$7_{757-765}$ (*bottom*) peptide, the cytotoxicity of the CTLs against T2 cells (HLA-A2$^+$, TAP deficient), pulsed with each peptide or peptide-unpulsed T2 cells, was detected by standard a ^{51}Cr release assay. These CTLs exhibited cytotoxicity to CDH3-$4_{655-663}$ (*top*) or CDH3-$7_{757-765}$ (*bottom*) peptide pulsed T2 cells, but not to peptide-unpulsed T2 cells. *B*, these CTLs exhibited cytotoxicity to the CDH3$^+$ HLA-A2$^+$ human colon cancer cell line HCT116 and oral squamous cancer cell line HSC3 and PANC1/CDH3, a CDH3$^-$ HLA-A2$^+$ human pancreatic cancer cell line PANC1 transfected with the human *CDH3* gene, but not to CDH3$^-$ HLA-A2$^+$ human liver cancer cell line SKHep1, PANC1, nor CDH3$^+$ HLA-A2$^-$ human pancreatic cancer cell line PK8. *C*, the CDH3-reactive CTLs generated from the PBMCs of HLA-A2– positive pancreatic and gastric cancer patients exhibited cytotoxicity to HCT116, PANC1/CDH3, and SKHep1/CDH3, a CDH3$^-$ HLA-A2$^+$ human liver cancer cell line SKHep1 transfected with the human *CDH3* gene, but not to PANC1, SKHep1, nor PK8. *D*, inhibition of cytotoxicity by anti–HLA class I mAb. After the target cells, SKHep1/CDH3 and HSC3 were incubated with anti–HLA class I mAb (W6/32, IgG2_a) or anti–HLA-DR mAb (H-DR-1, IgG2_a), respectively, for 1 h, the CTLs generated from the PBMCs of healthy donor by stimulation with CDH3-$4_{655-663}$ (*middle left*) or CDH3-$7_{757-765}$ (*right*) peptide were added. IFN-γ production (*left and right*; IFN-γ ELISPOT assay) and cytotoxicity (*middle*; ^{51}Cr release assay) were markedly inhibited by W6/32, but not by H-DR-1.

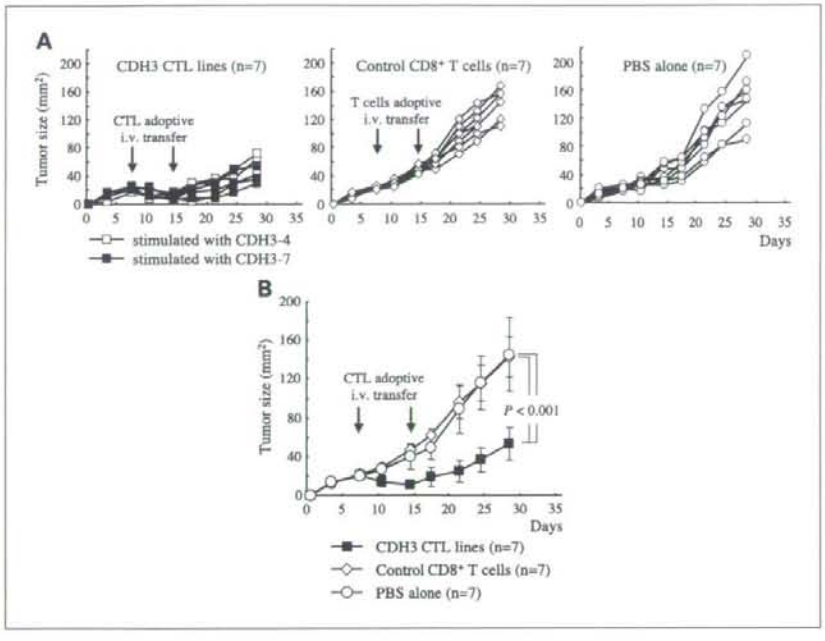

Fig. 5. *In vivo* antitumor activity of the CDH3-induced human CTLs adoptively transferred into NOD/SCID mice transplanted with human cancer cells. *A*, marked inhibition of growth of a human colorectal cancer cell line, HCT116 (CDH3$^+$, HLA-A2$^+$), engrafted into NOD/SCID mice after the adoptive CTL transfer. When the tumor size reached 25 mm^2 on day 7 after s.c. tumor implantation, human CTLs (4×10^6) reactive to CDH3-$4_{655\text{-}663}$ (□) and to CDH3-$7_{757\text{-}765}$ (■) peptide were inoculated i.v. On day 14, the same CTL inoculation was repeated. The control CD8$^+$ T cells stimulated with irrelevant HLA-A2–restricted HIV peptide (◇), which did not show cytotoxicity against HCT116 *in vitro*, were also inoculated into mice as a control. Tumor volumes in NOD/SCID mice given twice, on days 7 and 14, with CDH3-induced CTLs ($n = 7$), control CD8$^+$ T cells ($n = 7$), or PBS alone (○, $n = 7$). Tumor size is expressed in square millimeters. *B*, comparison of mean tumor sizes in each group of mice; bars, SD ($n = 7$).

HLA-A2–restricted mouse CTLs by the vaccination of HLA-A2.1 (HHD) Tgm with the 18 candidate peptides predicted by the BIMAS algorithm. Furthermore, we found that the CDH3-reactive CTLs could be generated from PBMCs stimulated with these peptides in healthy donors and cancer patients (Fig. 4). These CTLs could kill not only the T2 cells pulsed with its corresponding peptide but also the cancer cell lines expressing CDH3 in an HLA-A2–restricted manner. These data suggest that these CDH3 peptides (CDH3-$4_{655\text{-}663}$ and CDH3-$7_{757\text{-}765}$) are naturally processed from CDH3 protein in cancer cells and presented onto the cell surface together with HLA-A2 molecules to be recognized by the CTLs.

HLA-A2 (*A*0201*) is one of the most common *HLA* alleles in various ethnic groups, including Asians, Africans, Afro-Americans, and Caucasians (48). The identification of the HLA-A2–restricted and CDH3-derived CTL epitopes has also been suggested to be useful for the immunotherapy of many patients with pancreatic cancer all over the world.

We confirmed the cytotoxicity of the CDH3-reactive CTLs not only *in vitro* by a ^{51}Cr release assay but also *in vivo* by a CTL adoptive transfer model. As shown in Fig. 5, we observed that i.v. transferred CTLs inhibited the growth of tumor cells engrafted into NOD/SCID mice compared with the mice injected with control CD8$^+$ T cells or PBS alone. Although the inhibition of tumor growth was observed for a while after the i.v. transfer of the CTLs, thereafter, the tumor gradually enlarged. We thought that it was important to continue the transfer of the CTLs again and again to obtain the continuous regression of the tumor. These data suggest that the adoptive transfer of CDH3-reactive human CTLs into mice bearing human tumors expressing CDH3 could effectively inhibit tumor growth, at least in the NOD/SCID mouse tumor model.

It is considered to be very important to investigate whether the targeting CDH3 could induce autoimmune diseases, either during or after anticancer immunotherapy. After performing vaccinations twice with the epitope peptides identified in this study, we checked the autoimmune phenomenon in HLA-A2.1 (HHD) Tgm. As a result, any clinical symptoms, such as weight loss, diarrhea, or skin abnormalities, or any pathologic changes, such as lymphocyte infiltration or tissue destruction, were not observed (data not shown). However, the amino acid sequences of these two epitope peptides are not conserved between human and mouse CDH3. There is one amino acid replacement between human and mouse CDH3-$4_{655\text{-}663}$ peptide (human, FILPVLGAV; mouse, FILPILGAV) and CDH3-$7_{757\text{-}765}$ peptide (human, FIIENLKAA; mouse, FIIENLKPA). Therefore, we could not accurately check the capacity of autoimmune disease-inducing activity of two CDH3-derived peptides in our mouse system.

In conclusion, our results suggest that CDH3 is a novel TAA of which epitope peptides could elicit CTLs to cancer cells expressing CDH3 in an HLA-A2–restricted manner. As CDH3 is highly expressed in a wide range of human malignancies, including pancreatic cancer, CDH3 is therefore suggested to be a promising target of peptide-based immunotherapy for a broad spectrum of malignancies, without causing any autoimmune phenomena.

Disclosure of Potential Conflicts of Interest

No potential conflicts of interest were disclosed.

Acknowledgments

The authors thank Dr. Hideyuki Saya (Keio University), the Cell Resource Center for Biomedical Research Institute of Development, Aging and Cancer, Tohoku University, and the Health Science Research Resources Bank for providing the cell lines and Dr. Hiroyuki Miyoshi (Riken BioResource Center) for providing the lentiviral vector.

References

1. Jemal A, Siegel R, Ward E, Murray T, Xu J, Thun MJ. Cancer statistics 2007. CA Cancer J Clin 2007;57:43–66.
2. Sener SF, Fremgen A, Menck HR, Winchester DP. Pancreatic cancer: a report of treatment and survival trends for 100,313 patients diagnosed from 1985–1995, using the National Cancer Database. J Am Coll Surg 1999;189:1–7.
3. Eloubeidi MA, Desmond RA, Wilcox CM, et al. Prognostic factors for survival in pancreatic cancer: a population-based study. Am J Surg 2006;192:322–9.
4. Goonetilleke KS, Siriwardena AK. Nationwide questionnaire survey of the contemporary surgical management of pancreatic cancer in the United Kingdom and Ireland. Int J Surg 2007;5:147–51.
5. Smeenk HG, Tran TC, Erdmann J, van Eijck CH, Jeekel J. Survival after surgical management of pancreatic adenocarcinoma: does curative and radical surgery truly exist? Langenbecks Arch Surg 2005;390:94–103.
6. Yeo CJ, Cameron JL, Lillemoe KD, et al. Pancreaticoduodenectomy for cancer of the head of the pancreas. 201 patients. Ann Surg 1995;221:721–31.
7. Lockhart AC, Rothenberg ML, Berlin JD. Treatment for pancreatic cancer: current therapy and continued progress. Gastroenterology 2005;128:1642–54.
8. Boon T, van der Bruggen P. Human tumor antigens recognized by T lymphocytes. J Exp Med 1996;183:725–9.
9. van der Bruggen P, Traversari C, Chomez P, et al. A gene encoding an antigen recognized by cytolytic T lymphocytes on a human melanoma. Science 1991;254:1643–7.
10. Ito M, Shichijo S, Tsuda N, et al. Molecular basis of T cell-mediated recognition of pancreatic cancer cells. Cancer Res 2001;61:2038–46.
11. Chen YT, Scanlan MJ, Sahin U, et al. A testicular antigen aberrantly expressed in human cancers detected by autologous antibody screening. Proc Natl Acad Sci U S A 1997;94:1914–8.
12. Tureci O, Sahin U, Zwick C, Koslowski M, Seitz G, Pfreundschuh M. Identification of a meiosis-specific protein as a member of the class of cancer/testis antigens. Proc Natl Acad Sci U S A 1998;95:5211–6.
13. Nakatsura T, Senju S, Ito M, Nishimura Y, Itoh K. Cellular and humoral immune responses to a human pancreatic cancer antigen, coactosin-like protein, originally defined by the SEREX method. Eur J Immunol 2002;32:826–6.
14. Monji M, Senju S, Nakatsura T, et al. Head and neck cancer antigens recognized by the humoral immune system. Biochem Biophys Res Commun 2002;294:734–41.
15. Nakatsura T, Senju S, Yamada K, Jotsuka T, Ogawa M, Nishimura Y. Gene cloning of immunogenic antigens overexpressed in pancreatic cancer. Biochem Biophys Res Commun 2001;281:936–44.
16. Yoshitake Y, Nakatsura T, Monji M, et al. Proliferation potential-related protein, an ideal esophageal cancer antigen for immunotherapy, identified using complementary DNA microarray analysis. Clin Cancer Res 2004;10:6437–48.
17. Uchida N, Tsunoda T, Wada S, Furukawa Y, Nakamura Y, Tahara H. Ring finger protein 43 as a new target for cancer immunotherapy. Clin Cancer Res 2004;10:8577–86.
18. Suda T, Tsunoda T, Uchida N, et al. Identification of secernin 1 as a novel immunotherapy target for gastric cancer using the expression profiles of cDNA microarray. Cancer Sci 2006;97:411–9.
19. Watanabe T, Suda T, Tsunoda T, et al. Identification of immunoglobulin superfamily 11 (IGSF11) as a novel target for cancer immunotherapy of gastrointestinal and hepatocellular carcinomas. Cancer Sci 2005;96:498–506.
20. Nakatsura T, Komori H, Kubo T, et al. Mouse homologue of a novel human oncofetal antigen, glypican-3, evokes T-cell-mediated tumor rejection without autoimmune reactions in mice. Clin Cancer Res 2004;10:8630–40.
21. Komori H, Nakatsura T, Senju S, et al. Identification of HLA-A2- or HLA-A24-restricted CTL epitopes possibly useful for glypican-3-specific immunotherapy of hepatocellular carcinoma. Clin Cancer Res 2006;12:2689–97.
22. Nose A, Takeichi M. A novel cadherin cell adhesion molecule: its expression patterns associated with implantation and organogenesis of mouse embryos. J Cell Biol 1986;103:2649–58.
23. Wheelock MJ, Johnson KR. Cadherins as modulators of cellular phenotype. Annu Rev Cell Dev Biol 2003;19:207–35.
24. Behrens J. Cadherins and catenins: role in signal transduction and tumor progression. Cancer Metastasis Rev 1999;18:15–30.
25. Shimoyama Y, Hirohashi S, Hirano S, et al. Cadherin cell-adhesion molecules in human epithelial tissues and carcinomas. Cancer Res 1989;49:2128–33.
26. Palacios J, Benito N, Pizarro A, et al. Anomalous expression of P-cadherin in breast carcinoma. Correlation with E-cadherin expression and pathological features. Am J Pathol 1995;146:605–2.
27. Paredes J, Albergaria A, Oliveira JT, Jeronimo C, Milanezi F, Schmitt FC. P-cadherin overexpression is an indicator of clinical outcome in invasive breast carcinomas and is associated with CDH3 promoter hypomethylation. Clin Cancer Res 2005;11:5869–77.
28. Peralta Soler A, Knudsen KA, Salazar H, Han AC, Keshgegian AA. P-cadherin expression in breast carcinoma indicates poor survival. Cancer 1999;86:1263–72.
29. Stefansson IM, Salvesen HB, Akslen LA. Prognostic impact of alterations in P-cadherin expression and related cell adhesion markers in endometrial cancer. J Clin Oncol 2004;22:1242–52.
30. Nakamura T, Furukawa Y, Nakagawa H, et al. Genome-wide cDNA microarray analysis of gene expression profiles in pancreatic cancers using populations of tumor cells and normal ductal epithelial cells selected for purity by laser microdissection. Oncogene 2004;23:2385–400.
31. Pascolo S, Bervas N, Ure JM, Smith AG, Lemonnier FA, Perarnau B. HLA-A2.1-restricted education and cytolytic activity of $CD8^+$ T lymphocytes from $\beta 2$ microglobulin ($\beta 2m$) HLA-A2.1 monochain transgenic $H\text{-}2D^b$ $\beta 2m$ double knockout mice. J Exp Med 1997;185:2043–51.
32. Firat H, Garcia-Pons F, Tourdot S, et al. H-2 class I knockout, HLA-A2.1-transgenic mice: a versatile animal model for preclinical evaluation of antitumor immunotherapeutic strategies. Eur J Immunol 1999;29:3112–21.
33. Nakatsura T, Kageshita T, Ito S, et al. Identification of glypican-3 as a novel tumor marker for melanoma. Clin Cancer Res 2004;10:6612–21.
34. Nakatsura T, Yoshitake Y, Senju S, et al. Glypican-3, overexpressed specifically in human hepatocellular carcinoma, is a novel tumor marker. Biochem Biophys Res Commun 2003;306:16–25.
35. Tahara-Hanaoka S, Sudo K, Ema H, Miyoshi H, Nakauchi H. Lentiviral vector-mediated transduction of murine CD34(-) hematopoietic stem cells. Exp Hematol 2002;30:11–7.
36. Miyoshi H, Blomer U, Takahashi M, Gage FH, Verma IM. Development of a self-inactivating lentivirus vector. J Virol 1998;72:8150–7.
37. Gomi S, Nakao M, Niiya F, et al. A cyclophilin B gene encodes antigenic epitopes recognized by HLA-A24-restricted and tumor-specific CTLs. J Immunol 1999;163:4994–5004.
38. Kitahara O, Furukawa Y, Tanaka T, et al. Alterations of gene expression during colorectal carcinogenesis revealed by cDNA microarrays after laser-capture microdissection of tumor tissues and normal epithelia. Cancer Res 2001;61:3544–9.
39. Hasegawa S, Furukawa Y, Li M, et al. Genome-wide analysis of gene expression in intestinal-type gastric cancers using a complementary DNA microarray representing 23,040 genes. Cancer Res 2002;62:7012–7.
40. Kikuchi T, Daigo Y, Katagiri T, et al. Expression profiles of non-small cell lung cancers on cDNA microarrays: identification of genes for prediction of lymph-node metastasis and sensitivity to anti-cancer drugs. Oncogene 2003;22:2192–205.
41. Obama K, Ura K, Li M, et al. Genome-wide analysis of gene expression in human intrahepatic cholangiocarcinoma. Hepatology 2005;41:1339–48.
42. Frixen UH, Behrens J, Sachs M, et al. E-cadherin-mediated cell-cell adhesion prevents invasiveness of human carcinoma cells. J Cell Biol 1991;113:173–5.
43. Berx G, Staes K, van Hengel J, et al. Cloning and characterization of the human invasion suppressor gene E-cadherin (CDH1). Genomics 1995;26:281–9.
44. Oka H, Shiozaki H, Kobayashi K, et al. Expression of E-cadherin cell adhesion molecules in human breast cancer tissues and its relationship to metastasis. Cancer Res 1993;53:1696–701.
45. Suyama K, Shapiro I, Guttman M, Hazan RB. A signaling pathway leading to metastasis is controlled by N-cadherin and the FGF receptor. Cancer Cell 2002;2:301–14.
46. Taniuchi K, Nakagawa H, Hosokawa M, et al. Overexpressed P-cadherin/CDH3 promotes motility of pancreatic cancer cells by interacting with p120ctn and activating rho-family GTPases. Cancer Res 2005;65:3092–9.
47. Rosenberg SA, Yang JC, Restifo NP. Cancer immunotherapy: moving beyond current vaccines. Nat Med 2004;10:909–15.
48. Browning M, Krausa P. Genetic diversity of HLA-A2: evolutionary and functional significance. Immunol Today 1996;17:165–70.

Activation of Antigen-Specific Cytotoxic T Lymphocytes by β_2-Microglobulin or TAP1 Gene Disruption and the Introduction of Recipient-Matched MHC Class I Gene in Allogeneic Embryonic Stem Cell-Derived Dendritic Cells[1]

Yusuke Matsunaga,*§ Daiki Fukuma,† Shinya Hirata,* Satoshi Fukushima,*§ Miwa Haruta,*§ Tokunori Ikeda,*§ Izumi Negishi,‡ Yasuharu Nishimura,* and Satoru Senju[2]*§

A method for the genetic modification of dendritic cells (DC) was previously established based on the in vitro differentiation of embryonic stem (ES) cells to DC (ES-DC). The unavailability of human ES cells genetically identical to the patients will be a problem in the future clinical application of this technology. This study attempted to establish a strategy to overcome this issue. The TAP1 or β_2-microglobulin (β_2m) gene was disrupted in 129 (H-2^b)-derived ES cells and then expression vectors for the H-2K^d or β_2m-linked form of K^d (β2m-K^d) were introduced, thus resulting in two types of genetically engineered ES-DC, TAP1$^{-/-}$/K^d ES-DC and β_2m$^{-/-}$/β_2m-K^d ES-DC. As intended, both of the transfectant ES-DC expressed K^d but not the intrinsic H-2^b haplotype-derived MHC class I. β_2m$^{-/-}$/β_2m-K^d and TAP1$^{-/-}$/K^d ES-DC were not recognized by pre-activated H-2^b-reactive CTL and did not prime H-2^b reactive CTL in vitro or in vivo. β_2m$^{-/-}$/β_2m-K^d ES-DC and TAP1$^{-/-}$/K^d ES-DC had a survival advantage in comparison to β_2m$^{+/-}$/β_2m-K^d ES-DC and TAP1$^{+/+}$/K^d ES-DC, when transferred into BALB/c mice. K^d-restricted RSV-M2-derived peptide-loaded ES-DC could prime the epitope-specific CTL upon injection into the BALB/c mice, irrespective of the cell surface expression of intrinsic H-2^b haplotype-encoded MHC class I. β_2m$^{-/-}$/β_2m-K^d ES-DC were significantly more efficient in eliciting immunity against RSV M2 protein-expressing tumor cells than β_2m$^{+/-}$/β_2m-K^d ES-DC. The modification of the β_2m or TAP gene may therefore be an effective strategy to resolve the problem of HLA class I allele mismatch between human ES or induced pluripotent stem cells and the recipients to be treated. *The Journal of Immunology,* **2008, 181: 6635–6643.**

An efficient means for the activation of the CTL reactive to tumor Ags is crucial for T cell-mediated antitumor immunotherapy (1). Dendritic cells (DC)[3] are potent T cell stimulators and cellular vaccination using Ag-loaded DC has proven to be an efficient means for priming CTL specific to Ags (2, 3). This laboratory and others have established methods to generate DC from mouse and human embryonic stem (ES) cells (4–8). The capacity of ES cell-derived DC (ES-DC or esDC) to simulate alloreactive T cells and to prime Ag-specific CTL is comparable to that of conventional bone marrow-derived DC (BM-DC). Genetically modified ES-DC can be readily generated by introducing expression vectors into ES cells and the subsequent induction of their differentiation into ES-DC (9). The transfection of ES cells can be done by electroporation with plasmid vectors and the use of virus-based vectors is not necessary. Once an ES cell clone with proper genetic modification is established, it then serves as an infinite source for genetically modified DC. Mouse models have demonstrated that vaccination with genetically engineered ES-DC expressing tumor Ags (10) and T cell-attracting chemokines (11) is very effective for the induction of antitumor immunity.

In the future, the clinical application of ES-DC technology will require a solution to the problem of histoincompatibility between patients to be treated and the ES-DC. Specifically, the HLA allele mismatch may cause a rapid immune response and rejection of the inoculated cells (12), although a discrepancy in the minor histocompatibility Ag can also be a cause of alloreaction (13). The present study addressed this problem by using the strategy of modification of the genes that control the cell surface expression of MHC class I, i.e., β_2-microglobulin (β_2m) and TAP. TAP1$^{-/-}$ and β_2m$^{-/-}$ ES cell clones were generated from the ES cell lines derived from the 129 mouse (H-2^b) embryo. The expression vectors for H-2K^d and β_2m-linked form of H-2K^d (β2m-K^d) were then introduced into TAP1$^{-/-}$ and β_2m$^{-/-}$ ES cell clones, respectively. Subsequently, these genetically modified ES cells were subjected to a differentiation culture to generate ES-DC. The MHC class I molecules encoded by the genes in the H-2^b haplotype were either absent or at very low levels on the cell surface of these genetically modified ES-DC. The effect of the alteration of cell

*Department of Immunogenetics and †Department of Oral and Maxillofacial Surgery, Kumamoto University, Graduate School of Medical Sciences, Kumamoto, Japan; ‡Department of Dermatology, Gunma University Graduate School of Medicine, Gunma, Japan; and §Japan Science and Technology Agency, CREST, Tokyo, Japan

Received for publication July 10, 2008. Accepted for publication August 20, 2008.

The costs of publication of this article were defrayed in part by the payment of page charges. This article must therefore be hereby marked *advertisement* in accordance with 18 U.S.C. Section 1734 solely to indicate this fact.

[1] This work was supported in part by Grants-in-Aid 16590988, 17390292, 17015035, 18014023, 19591172, and 19059012 from the Ministry of Education, Culture, Sports, Science and Technology (MEXT), Japan; the Program of Founding Research Centers for Emerging and Reemerging Infectious Diseases launched as a project commissioned by MEXT, Japan; Research Grant for Intractable Diseases from Ministry of Health and Welfare, Japan; and grants from Japan Science and Technology Agency (JST), the Uehara Memorial Foundation, and the Takeda Science Foundation.

[2] Address correspondence and reprint requests to Dr. Satoru Senju, Department of Immunogenetics, Graduate School o f Medical Sciences, Kumamoto University, Honjo 1-1-1, Kumamoto, Japan. E-mail address: senjusat@gpo.kumamoto-u.ac.jp

[3] Abbreviations used in this paper: DC, dendritic cell; ES cell, embryonic stem cell; ES-DC, embryonic stem cell-derived DC; BM-DC, bone marrow-derived DC; β_2-microglobulin, β_2m; HA, hemagglutinin; RSV, respiratory syncytical virus; PEF, primary mouse embryonic fibroblast; CMTR, chloromethyl-benzoyl-amino-tetramethylrhodamine; CMFDA, chloromethylfluorescein diacetate; iPS cell, induced pluripotent stem cell; Luc, luciferase; IRES, Internal ribosomal entry site.

 0022-1767/08/$2.00

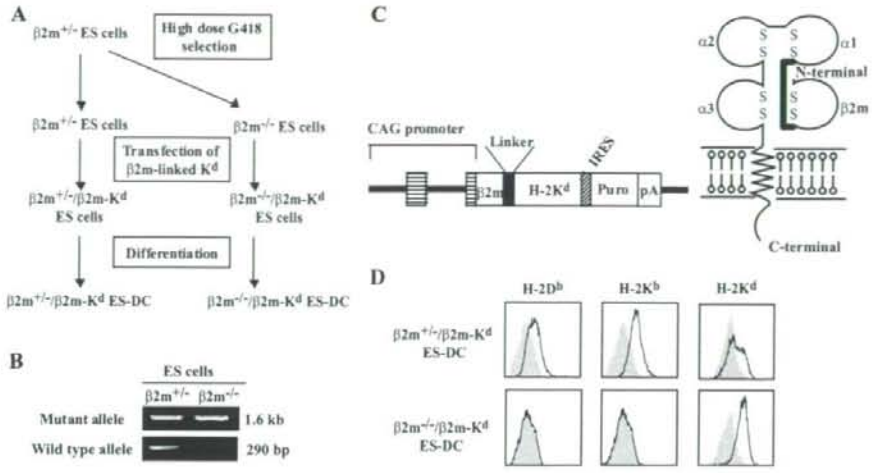

FIGURE 1. Generation of ES-DC deficient in the intrinsic β_2m gene and expressing recipient-matched MHC class I linked to β_2m. *A*, Overview of the method for generation of ES-DC-expressing β_2m-linked K^d, $\beta_2m^{+/-}/\beta_2$m-K^d ES-DC and $\beta_2m^{-/-}/\beta_2$m-K^d ES-DC. $\beta_2m^{-/-}$ ES cells were generated from $\beta_2m^{+/-}$ ES cells by high dose G418 selection. $\beta_2m^{+/-}$ and $\beta_2m^{-/-}$ ES cells were introduced with cDNA for the β2m-linked form of K^d and subsequently differentiated to generate $\beta2m^{+/-}/\beta$2m-K^d ES-DC and $\beta2m^{-/-}/\beta$2m-K^d ES-DC. *B*, The absence of wild-type β_2m gene in the $\beta_2m^{-/-}$ ES cell clone was confirmed by genomic PCR. *C*, Structure of the expression vector for β_2m-linked H-$2K^d$ (*left*) and a schematic representation of the encoded molecule (*right*). The β_2m was fused to H-$2K^d$ via a flexible 15 amino acid-long linker ($[Gly_4\text{-}Ser]_3$). The vector is driven by CAG promoter (pCAG) and cDNA for β_2m-linked H-$2K^d$ are followed by the IRES-puromycin-resistance gene ($Puro^R$)-polyadenylation signal sequence (pA). *D*, Analysis of the cell surface expression of MHC class I on ES-DC by flow cytometry. The staining patterns with specific Abs (thick lines) and isotype-matched controls (gray) are shown.

surface expression of MHC class I on activation of alloreactive (H-2^b haplotype-encoded MHC class I-reactive) CTL was analyzed in both in vitro and in vivo experiments. After loading ES-DC with the antigenic peptide having a capacity to bind H-$2K^d$ molecule, these ES-DC were transferred into BALB/c mice (H-2^d haplotype) to determine whether the peptide-specific, H-$2K^d$-restricted CTL could be primed in the recipient mice and whether Ag-specific antitumor immunity could be induced.

Materials and Methods

Mice

Six- to eight-week-old female BALB/c and 129/Sv (129) mice were purchased from Japan SLC and Clea Japan, respectively. The mice were housed at the Center for Animal Resources and Development (CARD, Kumamoto University) under specific pathogen-free conditions. All studies were performed under the approval of the animal experiment committee of Kumamoto University.

Peptides and cell lines

The respiratory syncytial virus (RSV) $M2_{82-90}$ epitope (SYIGSINNI) restricted to H-$2K^d$ has been described previously (14). H-$2K^d$-restricted HIV gag protein-derived $p24_{199-207}$ epitope (AMQMLKETI) was used as an irrelevant control peptide (15). The peptides were commercially synthesized and supplied at >98% purity (Anygen). Murine mastcytoma P815 cells were used as target cells for a ^{51}Cr release assay. A RSV-M2-transduced colon26/luciferase (Luc) cell line (colon26/M2-Luc) was established by the transfection of murine adenocarcinoma colon26 cells with an influenza virus hemagglutinin (HA)-tagged RSV M2 expression vector (pCAG-M2- internal ribosomal entry site (IRES)-neo^R) and a firefly luciferase expression vector (pCAG-luc-IRES-$puro^R$) by electroporation. After the transfection, G418 and puromycin were added to the culture medium for selection and single clones were obtained by limiting dilution. The expression of firefly luciferase was verified by measuring the luciferase activity in the cell lysates as described below. The expression of the HA-RSV-M2 protein in the selected transfectant clones was confirmed by a flow cytometric analysis following intracellular anti-HA staining and also using ELISA detecting IFN-γ-production by $M2_{82-90}$ specific K^d-restricted CTL cocultured with the transfectants.

Generation of TAP1- or β_2m-deficient ES cells and differentiation of DC from ES cells

ES cells were cultured on primary mouse embryonic fibroblast (PEF) feeder layers in complete ES cell medium, DMEM containing 20% Knock-Out Serum Replacement (Invitrogen Life Technologies), 2-ME (50 μM), and mouse leukemia inhibitory factor (1000 U/ml). A $\beta_2m^{+/-}$ ES cell clone established from D3 cell line derived from a 129 mouse embryo (H-2^b) was a generous gift from Dr. R. Jaenisch (Massachusetts Institute of Technology, Cambridge, MA) (16). To generate $\beta_2m^{-/-}$ ES cells, $\beta_2m^{+/-}$ ES cells (5×10^5 cells/90-mm culture dish) were cultured on feeder layers of neomycin-resistant PEF derived from GTPBP1$^{-/-}$ mouse embryos (17) in ES cell medium containing high dose G418 (1.5–2.0 mg/ml) for 10 days (18). After a further culture for 7 days without G418, the surviving ES cell colonies were picked up from the dishes, transferred to 24-well culture plates, and then expanded. For each isolated ES cell clones, a part of the expanded cells were cultured in gelatin-coated 6-well plates without PEF feeders. Genomic DNA extracted from the feeder-free ES cells was used for genotyping of the β_2m locus by genomic PCR and $\beta_2m^{-/-}$ ES clones were selected. TAP1$^{+/-}$ ES cells were generated from E14 ES cells derived from 129 mouse embryo (H-2^b). E14 cells were transfected with 30 μg of linearized targeting vector by electroporation (19). G418 and ganciclovir were added to the culture medium 24 h after the transfection and the surviving colonies were isolated during days 7–10 of selection. The isolated clones were analyzed by PCR and Southern blotting to identify cell clones with homologous recombination. Subsequently, one of the TAP1$^{+/-}$ clones was subjected to selection with high dose of G418 as in the case of $\beta2m^{-/-}$ ES cells. The clones were expanded and analyzed by Southern blotting to select TAP1$^{-/-}$ clones. Expression vectors for H-$2K^d$ and β_2m-linked form of H-$2K^d$ (β2m-K^d) were introduced into TAP1$^{-/-}$ and $\beta_2m^{-/-}$ ES cell clones, respectively. The induction of differentiation of ES cells into ES-DC was done as described previously (20). On day 17–19 of cultures, the floating or loosely adherent cells were recovered from culture dishes by pipeting and then were used for the experiments.

PCR

The initial screening of ES cells was done by PCR using the following primers: the wild type TAP1 allele (5′-ATGGGACACATGCACGGC-3′ and 5′-CCACAGTAGCAGGCTCAG-3′), the mutant TAP1 allele (5′-TG TAGCTTTGGCTCTTCTGGAA-3′ and 5′-GGGCCAGCTCATTCCTC CACTC-3′), β_2m (5′-CCTCAGAAACCCCTCAAATTCAAG-3′ and

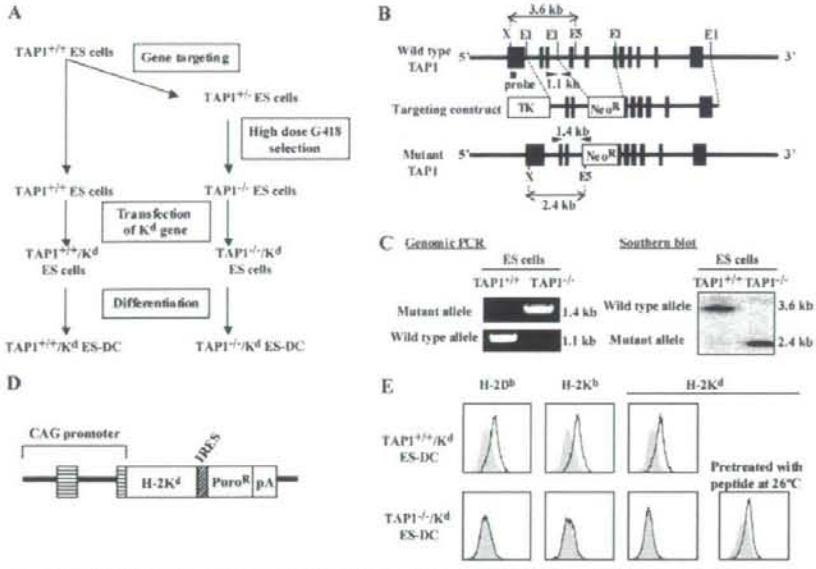

FIGURE 2. Generation of TAP1-deficient, recipient-matched MHC class I gene-introduced ES-DC. *A*, Overview of the method for generation of K^d expressing, TAP1-deficient ES-DC. $TAP1^{+/+}$ and $TAP1^{-/-}$ ES cells were transfected with cDNA for K^d and subsequently induced to differentiate into ES-DC. *B*, Structure of the mouse TAP1 genomic locus, the targeting construct and the mutant allele. Closed boxes indicate exons. The targeting construct contains a neomycin resistant gene (Neo^R) and herpesvirus thymidine kinase gene (TK). The sets of PCR primers for the wild-type allele and mutant allele are shown as arrowheads. The position of the probe used for the Southern blot analysis is indicated as a small black box. The sizes of bands generated from the wild-type and mutant allele by digestion with *Xho*I (X) and EcoR V (E5) are indicated. The EcoR I (E1) restriction site is also shown. *C*, A genotype analysis of ES cells. Genomic DNA from ES cells was analyzed by genomic PCR and Southern blotting. *D*, Structure of the H-$2K^d$ expression construct. The vector is driven by a CAG promoter (pCAG) and cDNA for H-$2K^d$ are followed by the IRES-puromycin-resistance gene ($Puro^R$)-polyadenylation signal sequence (pA). *E*, Surface phenotypes of genetically modified ES-DC. The surface expression of indicated MHC class I molecules on ES-DC were analyzed using flow cytometry. The expression of cell surface H-$2K^d$ by $TAP1^{-/-}/K_d$ ES-DC were detected after cells were incubated with 10 μM H-$2K^d$-binding peptide (RSV $M2_{82-90}$) at 26°C for 12 h, subsequently incubated at 37°C for 4 h and stained with anti-H-$2K^d$ Ab. The staining patterns with specific Abs (thick lines) and isotype-matched controls (gray) are shown.

5′-GCTTACCCCAGTAGACGGTCTTGG-3′). The set of primers for β_2m was designed to amplify both the wild type and targeted loci.

Southern blot analysis

To analyze the genotype of ES cells, genomic DNA isolated from ES cells was digested with *Xho*I and EcoR V. The DNA fragments were separated by electrophoresis in 0.8% agarose gels. Subsequently, the DNA was transferred onto nylon membranes. Probes for the Southern blot analysis were obtained by PCR with sets of primers for TAP1 locus (5′-GACCA GACTCTGGACAGCTCAC-3′ and 5′-AAGGCAAGAGAGAATCAA GAG-3′) from the genomic DNA of ES cells. Labeling of probe DNA with ^{32}P-dCTP was done by using a Megaprime DNA Labeling Kit (GE Healthcare) and the standard Southern blot procedure was conducted.

Abs and flow cytometric analysis

FITC-conjugated anti-H-$2K^d$ (BD Pharmingen), H-$2K^b$ (Caltag Laboratories), and H-$2D^b$ (Caltag Laboratories) Abs were purchased from the indicated sources. A flow cytometric analysis was done on a FACScan flow cytometer (BD Biosciences) and the data analysis was performed using the CellQuest software program (BD Biosciences).

Preparation of BM-DC

Bone marrow cells prepared from BALB/c or 129 mice were cultured in RPMI 1640 medium supplemented with 10% FCS, 500 U/ml GM-CSF, and 50 μM 2-ME. On day 7 of the culture, the cells were recovered and used as BM-DC for the experiments.

Analysis of stimulation of BALB/c -derived H-2^b-reactive $CD8^+$ T cell lines by DC

To generate BALB/c (H-2^d)-derived H-2^b-reactive $CD8^+$ T cell lines, 5×10^6 BALB/c spleen cells were cultured with 2×10^6 irradiated 129 (H-2^b) spleen cells in 2 ml of RPMI 1640 medium supplemented with 10% FCS, 100 U/ml IL-2 and 50 μM 2-ME in a well of 24-well plates for 5 days (21) and after that $CD8^+$ T cells were isolated by using anti-CD8 magnetic beads (Miltenyi Biotec). The H-2^b-reactive $CD8^+$ T cells (1×10^3) were cultured with the indicated stimulator DC (5×10^3) for 16 h and the activation of T cells was detected by IFN-γ-production by using ELISPOT (BD Biosciences). For the analysis of the priming of alloreactive (H-2^b-reactive) $CD8^+$ T cells by ES-DC, BALB/c spleen cells (5×10^6) were cultured with irradiated ES-DC (2×10^6) for 5 days and then $CD8^+$ T cells were isolated as described above. The magnitude of priming of H-2^b-reactive $CD8^+$ T cells was analyzed by IFN-γ-production detected by ELISPOT upon coculture with 129 mice-derived BM-DC as stimulators.

Analysis of frequency of alloreactive CTL in ES-DC-injected mice

Spleen cells were isolated from naive BALB/c mice or those that received multiple ES-DC injections and $CD8^+$ T cells were isolated by using anti-CD8 magnetic beads (Miltenyi Biotech). To analyze the frequency of auto (H-2^d)- or allo (H-2^b)-reactive $CD8^+$ T cells, the cells (5×10^3) were cocultured with BALB/c or 129 BM-DC (5×10^3) for 16 h and IFN-γ producing cells were detected using the ELISPOT assay.

Detection of in vivo administered ES-DC in the draining lymph nodes

The in vivo elimination of ES-DC was assessed according to the reported procedures with some modification (22). In brief, ES-DC were labeled with the 10 μM chloromethyl-benzoyl-amino-tetramethyl-rhodamine (CMTMR; Molecular Probes) and BALB/c BM-DC were labeled with 10 μM chloromethylfluorescein diacetate (CMFDA; Molecular Probes) according to the manufacturer's instructions. The mice were injected s.c. in the forelimb with 2×10^6

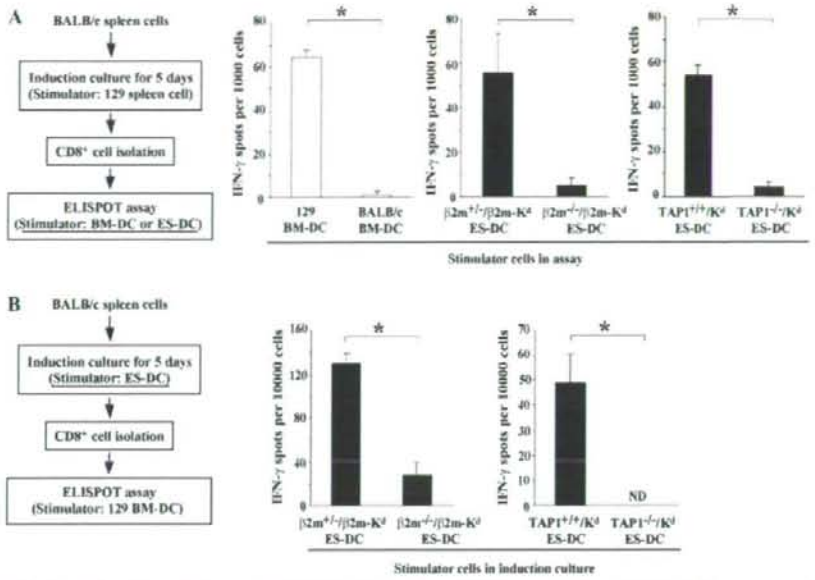

FIGURE 3. Reduced in vitro stimulation of alloreactive CD8$^+$ T cells by β_2m or TAP1 gene-deficient ES-DC. *A*, The response of H-2^b-reactive CD8$^+$ T cells to ES-DC was reduced by modification of the β_2m (*middle panel*) or TAP1 (*right panel*) gene. To generate alloreactive (anti-H-2^b) CTL, 5×10^6 BALB/c (H-2^d) spleen cells were cultured with 2×10^6 irradiated 129 (H-2^b) spleen cells for 5 days and after that the CD8$^+$ cells were purified from the culture. The alloreactive CD8$^+$ T cells (1×10^3) were cultured with the ES-DC (5×10^3) of the indicated genotype for 16 h. The 129 or BALB/c BM-DC were used as additional controls (*left panel*). The number of IFN-γ producing cells was measured using an ELISPOT assay. *B*, Allogeneic MHC class I-deficient ES-DC showed reduced potency to prime alloreactive CD8$^+$ T cells in vitro. Splenocytes (5×10^6) derived from BALB/c mice were cultured with irradiated ES-DC (2×10^6) of the indicated genotype for 5 days and after that CD8$^+$ T cells were purified from the culture. The IFN-γ producing response of the CD8$^+$ T cells was measured with an ELISPOT with 129 BM-DC as stimulators. The results of the experiments with β_2m deficient ES-DC (*left panel*) and TAP1-deficient ES-DC (*right panel*) are shown. Data are representative of at least two experiments with similar results. The data are the mean ± SD of triplicate assays. The asterisks indicate significant ($p < 0.05$, Student's *t* test) differences between the two groups. ND, not detectable.

cells containing equal numbers of CMTMR-labeled ES-DC and CMFDA-labeled BM-DC. After 48 h, the draining axillary and brachial lymph nodes were removed, digested with collagenase type II and DNase I and analyzed for the presence of fluorescent cells by flow cytometry. The number of ES-DC was normalized to control syngeneic BALB/c BM-DC.

Priming of RSV-M2 specific CD8$^+$ T cells by ES-DC

ES-DC were incubated with RSV-M2$_{82-90}$ peptide (10 μM) for 3 h and then washed three times with FCS-free DMEM. Ag-loaded ES-DC were injected i.p. (1×10^5 cells/injection/mouse) into the mice twice, with a 7-day interval. In some experiments, non-Ag-loaded ES-DC were injected five or ten times with 7-day intervals before the injection of Ag-loaded ES-DC. Seven days after the last injection of ES-DC, the mice were sacrificed and the spleen cells were isolated. After hemolysis, the spleen cells were cultured in the presence of M2$_{82-90}$ peptide (1 μM). Six days later, the cells were recovered and cytotoxic activity against M2$_{82-90}$ peptide pulsed-P815 target cells were measured using the standard ^{51}Cr- release assay.

Tumor challenge experiments

The mice were immunized with ES-DC and, 7 days after the immunization, colon26/M2-Luc (1×10^6/mouse) cells were injected into the mice i.p. Ten days later, the mice were sacrificed and the luciferase activity of the lysates of the abdominal organs was measured to quantify tumor growth. The tissue specimens were homogenized in 3 ml of lysis buffer (0.05% Triton X-100, 2 mM EDTA, 0.1 M Tris (pH 7.8)) and the homogenates were cleared by centrifugation at 10,000 × *g* for 5 min. Fifty μl of the supernatant was mixed with 50 μl of dilution buffer (PBS containing 2.4 mM $CaCl_2$ and 0.82 mM $MgSO_4$) and 100 μl of luciferase assay buffer (Steadyliteplus, PerkinElmer) and at 5 min after the mixing the light produced was measured for 1 second in a luminometer (Tristar LB941, Berthold Technologies).

Statistical analysis

Student's *t* test was used for the statistical analysis of data except for the data regarding the tumor invasion experiments. Because some of data in the tumor invasion experiments did not follow a normal distribution, the data were analyzed using the Mann-Whitney *U* test, a nonparametric test. A value of $p < 0.05$ was considered to be significant.

Results

Generation of ES-DC expressing recipient-matched MHC class I but not intrinsic MHC class I

The present study evaluated a strategy to prime Ag-specific CTL by transfer of genetically engineered 129 (H-2^b)-derived ES-DC into BALB/c (H-2^d) recipient mice, thus avoiding the recognition of ES-DC by allo (H-2^b)-reactive CD8$^+$ T cells. To modify the cell surface expression of MHC class I, two strategies were tested in parallel: 1) disruption of the β_2m gene in ES cells and introduction of β_2m-linked form of recipient-matched MHC class I (β_2m-K^d) (Fig. 1*A*), 2) disruption of TAP1 gene, introduction of recipient-matched MHC class I (K^d) and loading of K^d-binding epitopes to the ES-DC (Fig. 2*A*).

$\beta_2m^{-/-}$ ES cells were generated by the selection of the previously established $\beta_2m^{+/-}$ ES cells (16) with high dose (1.5–2 mg/ml) of G418. Two of the 39 clones were found to have a $\beta 2m^{-/-}$ genotype by genomic PCR (Fig. 1*B*). Subsequently, an expression vector for β_2m-K^d (Fig. 1*C*) was introduced into both $\beta_2m^{+/-}$ and $\beta_2m^{-/-}$ ES cells to generate $\beta_2m^{+/-}/\beta_2$m-K^d and $\beta_2m^{-/-}/\beta_2$m-K^d ES cells, respectively. The genetically modified ES cell clones were subjected to differentiation culture to generate ES-DC. Theoretically, β_2m-K^d is the only MHC class I molecule expressed on the cell surface of $\beta_2m^{-/-}/\beta_2$m-K^d ES-DC. In the flow cytometric analysis, the cell surface expression of MHC class I molecules of H-2^b haplotype, H-2D^b and K^b, was detected in $\beta_2m^{+/-}/\beta_2$m-K^d ES-DC but not in $\beta_2m^{-/-}$/

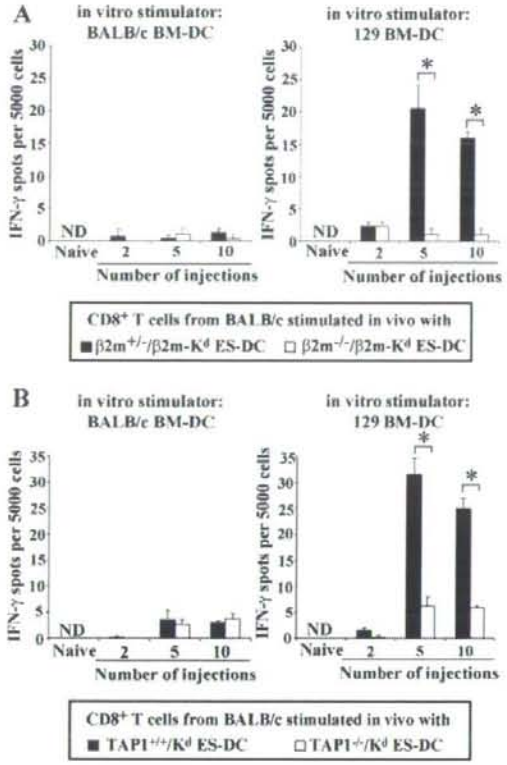

FIGURE 4. Reduced in vivo stimulation of alloreactive $CD8^+$ T cells by β_2m or TAP1 gene-modified ES-DC. Splenic $CD8^+$ T cells were isolated from naive BALB/c mice or those received multiple injections of β_2m deficient (*A*) or TAP1 deficient (*B*) ES-DC (1×10^5/injection). Isolated $CD8^+$ T cells (5×10^3) were cultured with BALB/c BM-DC (*left panels*) or 129 BM-DC (*right panels*) (5×10^3) for 16 h. The numbers of IFN-γ producing cells were measured using an ELISPOT assay. Data are representative of at least two experiments with similar results. The data are the mean ± SD of triplicate assays. Asterisks indicate significant ($p < 0.05$, Student's *t* test) differences. ND, not detectable.

β_2m-K^d ES-DC. Expression of K^d was detected in the both types of ES-DC, as expected (Fig. 1*D*).

To mutate the TAP1 gene in ES cells, the targeting vector (Fig. 2*B*) was introduced into E14 ES cells to make several $TAP1^{+/-}$ ES cell clones. Subsequently, one of the $TAP1^{+/-}$ clones was subjected to selection with high dose of G418 as in the case of $\beta_2m^{-/-}$ ES cells and $TAP1^{-/-}$ ES cell clones were isolated. Eight of the 88 surviving clones were found to be of $TAP^{-/-}$ genotype by genomic PCR (Fig. 2*C*, *left*) and Southern blotting (Fig. 2*C*, *right*). Next, an expression vector for K^d (Fig. 2*D*) was introduced into both $TAP1^{+/+}$ and $TAP1^{-/-}$ ES cells to generate $TAP1^{+/+}$/K^d and $TAP1^{-/-}$/K^d ES cells, respectively. Intrinsic MHC class I molecules, D^b and K^b, as well as transgene-derived K^d, were not detected on the cell surface of $TAP1^{-/-}$/K^d ES-DC (Fig. 2*E*). A low level of cell surface expression of K^d on $TAP1^{-/-}$/K^d ES-DC was observed after incubation of the ES-DC with K^d-binding peptide ($RSV\text{-}M2_{82\text{-}90}$) at 26°C for 12 h followed by the incubation at 37°C for 4 h (Fig. 2*E*).

Collectively, ES-DC expressing only transgene-derived K^d but not intrinsic ($H\text{-}2^b$ haplotype-derived) MHC class I molecules on the cell surface were generated by the two methods of genetic modifications of ES cells.

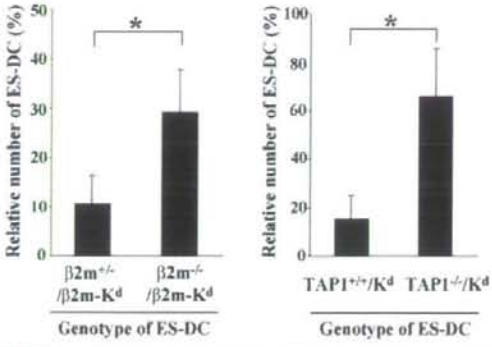

FIGURE 5. The survival advantage of β_2m or TAP1 gene-deficient ES-DC in allogeneic recipient mice. BALB/c mice were injected s.c. into the forelimb with CMFDA-labeled BALB/c BM-DC (1×10^6) and CMTMR-labeled ES-DC (1×10^6). After 48 h, the mice were killed and the number of labeled BM-DC and ES-DC in the axillary and brachial lymph nodes was determined by flow cytometry. The number of detected ES-DC was normalized to control syngeneic BALB/c BM-DC [(CMTMR$^+$ ES-DC/CMFDA$^+$ BM-DC) × 100]. The results of experiments with β_2m-deficient ES-DC (*left*) and TAP1-deficient ES-DC (*right*) are shown. Data are representative of two experiments with similar results. The data are the mean ± SD (5–6 mice per each group). Asterisks indicate significant ($p < 0.05$, Student's *t* test) differences.

Avoidance of recognition by alloreactive $CD8^+$ T cells by genetic modification of ES-DC

$H\text{-}2^b$ MHC class I-reactive $CD8^+$ T cells were prepared by a 5-day-culture of BALB/c ($H\text{-}2^d$) spleen cells with irradiated 129 ($H\text{-}2^b$) spleen cells. They produced IFN-γ in response to 129 mouse-derived BM-DC but not against BALB/c BM-DC, confirming that they responded specifically to $H\text{-}2^b$ MHC class I (Fig. 3*A*, *left panel*). The four types of ES-DC derived from $H\text{-}2^b$ ES cells with genetic modification described above were cocultured with the $H\text{-}2^b$-reactive $CD8^+$ T cell line and the activation of the T cells was analyzed. Fig. 3*A* shows that $\beta_2m^{+/-}/\beta_2$m-K^d ES-DC (*middle panel*) and $TAP1^{+/+}/K^d$ ES-DC (*right panel*), expressing MHC class I of $H\text{-}2^b$ haplotype along with K^d, were recognized by the $H\text{-}2^b$-reactive $CD8^+$ T cells, thus resulting in IFN-γ production at the magnitude similar to that observed in the case of 129 BM-DC. In contrast, $H\text{-}2^b$-reactive $CD8^+$ T cells showed practically no response to $\beta2m^{-/-}/\beta$2m-K^d ES-DC or $TAP1^{-/-}/K^d$ ES-DC. These results indicate that ES-DC that were not recognized by alloreactive $CD8^+$ T cells could be generated by the modification of β_2m or TAP1 gene to inhibit surface expression of intrinsic MHC class I molecules.

Reduced priming of $H\text{-}2^b$-reactive $CD8^+$ T cells in vitro by genetically modified ES-DC

Next, the in vitro priming of alloreactive $CD8^+$ T cells by ES-DC was examined. Spleen cells from BALB/c mice were cocultured with either of the four types of genetically engineered ES-DC for 5 days. After that, $CD8^+$ T cells were isolated from the culture and their reactivity to 129-derived BM-DC (Fig. 3*B*) was measured to assess the magnitude of priming in vitro of $H\text{-}2^b$-reactive $CD8^+$ T cells by the ES-DC. $CD8^+$ T cells cultured with $\beta_2m^{+/-}/\beta_2$m-K^d or $TAP1^{+/+}/K^d$ ES-DC in the induction phase responded to 129-derived BM-DC, indicating that both $\beta_2m^{+/-}/\beta_2$m-K^d and $TAP1^{+/+}/K^d$ ES-DC primed $H\text{-}2^b$-reactive $CD8^+$ T cells. In contrast, $CD8^+$ T cells cultured with $\beta_2m^{-/-}/\beta$2m-K^d or $TAP1^{-/-}/K^d$ ES-DC in the induction step exhibited reduced or no response to 129-derived BM-DC, thus

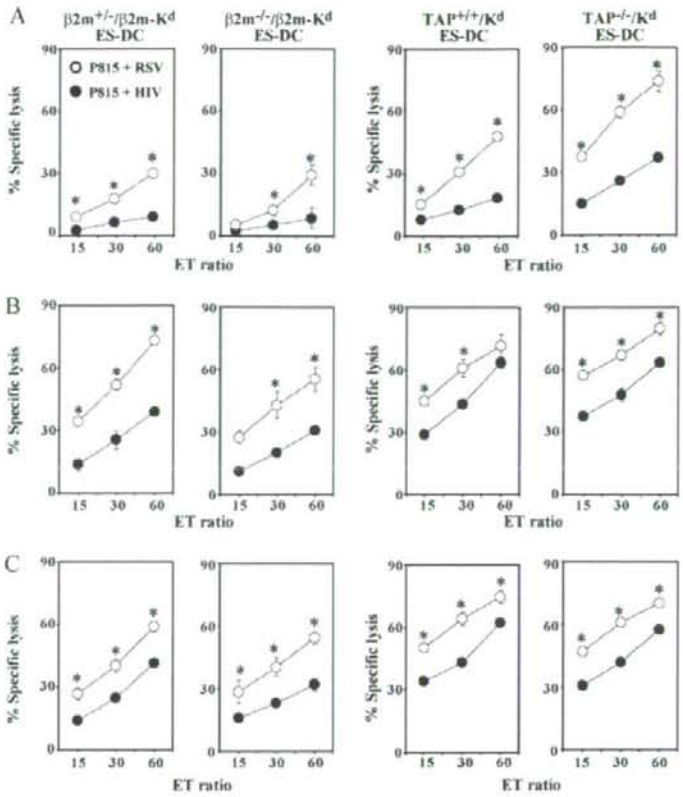

FIGURE 6. Priming of exogenous Ag-specific CTL by injection of genetically modified ES-DC loaded with antigenic peptide. *A*, RSV antigenic peptide-loaded ES-DC (1×10^5/injection/mouse) were injected i.p. into the naive mice twice with a 7-day interval. *B* and *C*, Non-Ag loaded ES-DC were injected 5 (*B*) or 10 (*C*) times with 7 days intervals before immunization with peptide-loaded ES-DC. The mice were sacrificed 7 days after the last injection of ES-DC and the spleen cells were isolated. The spleen cells were cultured in the presence of RSV peptide (1 μM) for 6 days and then analyzed on the RSV peptide-specific cytolytic activity by 5-h ^{51}Cr release assay. As target cells, P815 cells either pulsed with $M2_{82-90}$ peptide (○) or control H-2K^d-restricted HIV gag $p24_{199-207}$ peptide (●) were used. Data are representative of three experiments with similar results. The data are the mean specific lysis ± SD of triplicate assays. The asterisks indicate significant ($p < 0.05$, Student's t test) differences.

indicating that the H-2^b-reactive CD8$^+$ T cells had not been well primed. These results suggest that the in vitro priming of allo-MHC class I-reactive T cells by ES-DC can be reduced through the genetic modification of β_2m or TAP1.

Reduced priming of allo-MHC class I-reactive T cells in vivo by TAP1 or β_2m-deficient ES-DC

The next experiments assessed whether or not priming of alloreactive CD8$^+$ T cells upon in vivo administration of ES-DC could be avoided by the current strategy. The frequency of primed H-2^b-reactive CD8$^+$ T cells in mice was quantified by an ex vivo ELISPOT assay detecting the production of IFN-γ upon stimulation with 129-derived BM-DC. CD8$^+$ T cells from naive BALB/c mice showed little response to 129-derived BM-DC. CD8$^+$ T cells isolated from BALB/c mice injected 5 or 10 times with β_2m$^{+/-}$/β2m-K^d (Fig. 4*A*) or TAP1$^{+/+}$/K^d ES-DC (Fig. 4*B*) clearly responded, thus indicating the priming of H-2^b-reactive CD8$^+$ T cells. The magnitude of the response of the mice injected ten times was lower than those injected five times, in both the β2m$^{+/-}$/β_2m-K^d ES-DC and TAP1$^{+/+}$/K^d ES-DC-injected mice, thus suggesting that there is probably a limit in the frequency of alloreactive CD8$^+$ T cells. In contrast, the frequency of H-2^b-reactive CD8$^+$ T cells in mice inoculated with β_2m$^{-/-}$/β_2m-K^d or TAP1$^{-/-}$/K^d ES-DC was very low, indicating that alloreactive CD8$^+$ T cells were hardly primed in vivo by these ES-DC.

Surviving advantage of β_2m or TAP1 gene-modified ES-DC in vivo

According to a previous study by another group (23), BM-DC inoculated into allogeneic recipient mice are eliminated within a few days and the number of DC detected in the draining lymph node is lower than that of DC syngeneic to the recipient mice. In such circumstances, the rapid elimination of APC is mainly mediated by CD8$^+$ T cells reactive to allogeneic MHC class I (24). As described so far, the β_2m$^{-/-}$/β_2m-K^d ES-DC and TAP1$^{-/-}$/K^d ES-DC did not express intrinsic H-2^b-derived MHC class I molecule and escaped recognition by H-2^b-reactive CD8$^+$ T cells. Therefore, they were expected to have an advantage in surviving in allogeneic BALB/c mice, in comparison to ES-DC expressing H-2^b gene encoded MHC class I on the cell surface.

To examine the effect of genetic modification on the survival of ES-DC upon injection into allogeneic mice, equal numbers of CMTMR-labeled ES-DC and CMFDA-labeled BALB/c derived BM-DC, as a control, were mixed and injected in the right forelimb footpad of BALB/c mice. After 48 h, a single cell suspension was made from the axillary and brachial lymph nodes and the fluorochrome-labeled DC were detected by using flow cytometry (Fig. 5). The number of β_2m$^{-/-}$/β_2m-K^d ES-DC in the draining lymph nodes was ~3 times higher than that of β_2m$^{+/-}$/β_2m-K^d ES-DC. In the similar experiments, the number of detected TAP1$^{-/-}$/K^d ES-DC was ~4 times higher than that of TAP1$^{+/+}$/K^d ES-DC. These results suggest that ES-DC without cell surface expression of intrinsic MHC class I molecule can thus escape elimination by alloreactive CTL.

Priming of Ag-specific CTL by genetically modified ES-DC in allogeneic recipients

It has been noted that the CTL-mediated elimination of DC has a notable effect on the magnitude of immune responses in vivo (25) and the results so far described indicate that the β_2m or TAP1 gene-modified ES-DC expressing only recipient-matched MHC

class I could thus avoid elimination by CTL upon transfer into allogeneic recipients. Therefore, the ability of such ES-DC to elicit more robust Ag-specific immune responses in allogeneic recipients than ES-DC expressing intrinsic MHC class I was examined.

The priming of a RSV M2 protein epitope ($M2_{82-90}$)-specific and H-2K^d-restricted CTL by ES-DC administered into BALB/c mice was examined. $M2_{82-90}$ peptide-loaded ES-DC were injected i.p. into BALB/c mice twice with a 7-day interval. The spleen cells were isolated from the mice 7 days after the second injection and cultured in vitro in the presence of $M2_{82-90}$ peptide. After 6 days, the cultured spleen cells were recovered and assayed for their capacity to kill P815 mastcytoma cells (H-2^d) prepulsed with the M2 peptide. M2 peptide-specific and K^d-restricted CTL was primed in BALB/c mice immunized with either of the 4 types of genetically modified ES-DC (Fig. 6*A*). Therefore, ES-DC expressing K^d could prime K^d-restricted Ag-specific CTL, irrespective of cell surface expression of intrinsic MHC class I encoded by the H-2^b haplotype.

To determine whether or not ES-DC could prime $M2_{82-90}$ specific CTL in the presence of preprimed H-2^b-reactive CTL, ES-DC without peptide loading were injected in BALB/c mice five (Fig. 6*B*) or ten times (Fig. 6*C*) with 7-day intervals and then the same ES-DC loaded with $M2_{82-90}$ peptide were injected. In addition, in this case, the specific CTL were primed by all of the four types of ES-DC. These results indicate that even in the presence of preactivated alloreactive CTL, ES-DC expressing recipient-matched MHC class I are able to prime the Ag-specific CTL, whether or not the ES-DC express intrinsic MHC class I on their cell surface.

Induction of antitumor immunity by genetically modified ES-DC in allogeneic recipients

Next, antitumor immunity induced by the genetically modified ES-DC was assessed. To this end, a tumor cell line colon26/M2-Luc, a BALB/c-derived colon carcinoma cell line colon26 expressing RSV-M2 along with firefly luciferase, was generated. After the inoculation of the tumor cells, it was possible to quantify the number of cancer cells in mouse tissues by measuring the luciferase activity of tissue homogenates as reported (26). The luciferase activity in the homogenates of colon 26/M2-Luc cells was linearly correlated with the number of the cells in the range from 150 to 350,000 counts per second (Fig. 7*A*). In a pilot study, when the tumor cells were injected into the mice i.p., most tumor cells were detected in the greater omentum and the mesenterium, and the luciferase activity of these two organs were in parallel (data not shown). Therefore, the luciferase activity of the greater omentum was chosen to be measured in the following studies.

BALB/c mice were injected i.p. with ES-DC loaded with $M2_{82-90}$ peptide and other mice were injected with ES-DC prepulsed with irrelevant control peptide (HIV gag $p24_{199-207}$) with K^d-binding affinity. One week after the ES-DC injection, the mice were challenged i.p. with colon26/M2-Luc. After 10 days, the growth of tumor cells was evaluated by measuring the luciferase activity in the homogenate of the greater omentum. In the mice injected with either of the $\beta_2m^{-/-}/\beta$2m-K^d ES-DC (Fig. 7*B*) or TAP1$^{-/-}$/K^d ES-DC (Fig. 7*C*) loaded with M2 peptide, tumor growth was significantly reduced in comparison to the mice injected with the same ES-DC loaded with the control peptide. Therefore, the two types of genetically modified ES-DC could induce Ag-specific antitumor immunity. The antitumor effect induced by $\beta_2m^{-/-}/\beta_2$m-K^d ES-DC was significantly stronger than that induced by $\beta_2m^{+/-}/\beta_2$m-K^d ES-DC, indicating that the disruption of intrinsic β_2m gene and introduction of β_2m-linked MHC class I in ES-DC may provide an advantage in the induction of Ag-specific antitumor immunity.

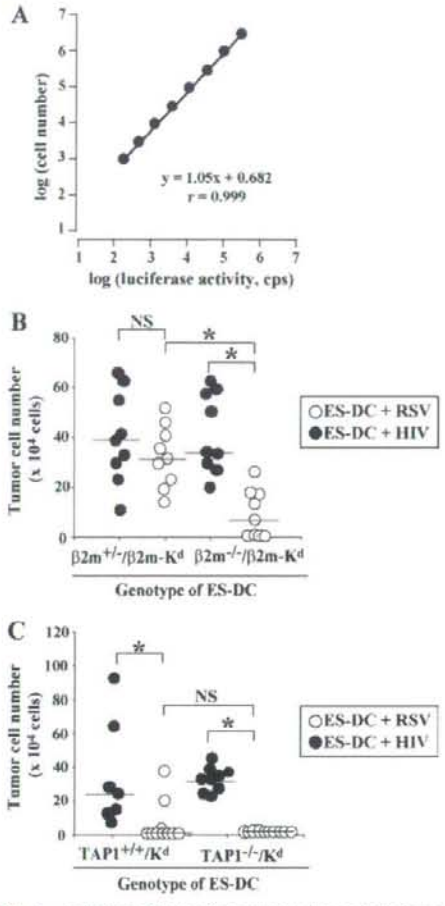

FIGURE 7. Induction of protective immunity by Ag-loaded genetically modified ES-DC against peritoneally disseminated tumor cells in allogeneic recipients. *A*, Homogenates were made from the indicated numbers of in vitro cultured colon26/M2-Luc cells and the luciferase activity was measured. r, correlation coefficient. *B* and *C*, BALB/c mice were injected with $M2_{82-90}$ peptide- or control HIV $p24_{199-207}$ peptide-loaded ES-DC (1×10^5/mouse) i.p. on day −7 and challenged with colon26/M2-Luc (1×10^6/mouse) i.p. on day 0. On day 10, the mice were sacrificed and luciferase activity of the greater omentum was measured. Luciferase activity of tissue lysates was converted to tumor cell number in the greater omentum based on the standard curve shown in *A*. The results of mice treated with $\beta_2m^{+/-}/\beta_2$m-K^d ES-DC or $\beta_2m^{-/-}/\beta_2$m-K^d ES-DC are shown in *B*. The results of mice treated with TAP1$^{+/+}$/K^d ES-DC or TAP1$^{-/-}$/K^d ES-DC are shown in *C*. All data are representative of at least two experiments with similar results. Values for individual mice injected with $M2_{82-90}$ peptide-loaded ES-DC (○) and HIV $p24_{199-207}$ peptide-loaded ES-DC (●) are shown; bars indicate median values. The asterisks indicate significant ($p < 0.05$) differences between two groups based on the Mann-Whitney *U* test. NS, not significant.

Discussion

To induce T cell-mediated anticancer immunity, vaccination with DC loaded with tumor Ag-derived peptides or tumor cell lysates are being clinically tested (27, 28). For such purposes, DC are generated from monocytes obtained from peripheral blood of the patients. However, monocytes are not easily propagated in vitro and apheresis, a procedure sometimes invasive for the patients, is necessary to obtain a sufficient number of monocytes as the source of DC. In addition, the culture to generate DC should be done

separately for each patient and for each treatment and thus the presently used method is too labor-intensive and costly to be broadly applied.

ES cells exhibit the remarkable properties of self-renewal and pluripotency. This capacity allows for the production of sizeable quantities of therapeutic cells of the hematologic lineage, including DC (29). If the ES-DC method is clinically applied, it will be possible to generate genetically engineered DC-expressing target Ags or immunostimulatory molecules, without use of virus-based vectors. However, considering the medical application, one drawback of the ES-DC method is the unavailability of human ES cells genetically identical to the patients to be treated (12). Specifically, an HLA allele mismatch between ES cells and patients is a crucial problem.

In previous studies, it was shown that allogeneic BM-DC are rapidly eliminated from the draining lymph nodes during the course of a primary alloreactive responses (23, 30). Another study revealed that the elimination of transferred APC in allogeneic recipients is mainly mediated by T cells reactive to allogeneic MHC class I but not MHC class II (24). Therefore, if the expression of the intrinsic MHC class I by ES-DC could be blocked, then ES-DC inoculated into allogeneic recipients would escape elimination by the alloreactive T cells of the recipients. However, the genomic region including the MHC class I genes spans more than 1,000 kb in both the mouse and human genome and complete elimination of such a large genomic region by gene-targeting technique is currently infeasible. The feasible candidates for genetic modification are the genes that encode β_2m and TAP, which regulate MHC class I expression (31, 32). Therefore, the present study adopted a strategy to block the cell surface expression of the MHC class I molecules by elimination of the β_2m or TAP1 gene.

Both alleles of the TAP1 or β_2m gene were disrupted in 129-derived ES cells (H-2^b) and subsequently expression vectors for the recipient (BALB/c)-matched K^d or β_2m-linked form of K^d were introduced. The genetically modified ES cells were subjected to the differentiation culture to generate TAP1$^{-/-}$/K^d ES-DC and $\beta_2m^{-/-}$/β_2m-K^d ES-DC. As intended, the $\beta_2m^{-/-}$/β_2m-K^d ES-DC expressed only K^d molecule as MHC class I molecules on the cell surface. TAP1$^{-/-}$/K^d ES-DC hardly expressed any classical MHC class I and a low level of cell surface expression of K^d was observed after incubation with K^d-binding peptide. In vitro, $\beta_2m^{-/-}$/β_2m-K^d and TAP1$^{-/-}$/K^d ES-DC were not recognized by pre-activated H-2^b-reactive CD8 T^+ cells and the ES-DC did not prime H-2^b-reactive $CD8^+$ T cells (Fig. 3). When these cells were inoculated into BALB/c mice, they did not prime H-2^b reactive $CD8^+$ T cells in vivo (Fig. 4).

Consistent with these results, $\beta_2m^{-/-}$/β2m-K^d ES-DC and TAP1$^{-/-}$/K^d ES-DC had a survival advantage in comparison to $\beta_2m^{+/-}$/β_2m-K^d ES-DC and TAP1$^{+/+}$/K^d ES-DC, when transferred into BALB/c mice (Fig. 5). The results suggest that ES-DC deficient in β_2m or TAP1 and expressing only recipient-matched MHC class I were resistant to elimination by alloreactive CTL. It has been shown that CTL-mediated elimination of DC has a notable effect on the magnitude of immune responses in vivo (25, 33). Therefore, β_2m- or TAP1-deficient ES-DC should be able to elicit more robust priming of Ag-specific CTL in allogeneic recipients than ES-DC expressing intrinsic MHC class I. When loaded with RSV-derived peptide and inoculated into BALB/c mice, not only $\beta_2m^{-/-}$/β_2m-K^d and TAP1$^{-/-}$/K^d ES-DC but also $\beta_2m^{+/-}$/β_2m-K^d and TAP1$^{+/+}$/K^d ES-DC primed K^d-restricted, RSV peptide-specific CTL (Fig. 6). Unexpectedly, there was no significant difference in the magnitude of priming of Ag-specific CTL among these ES-DC. CTL-mediated allogeneic DC elimination is mainly dependent on the perforin/granzyme B pathway (24, 30). Therefore, the result shown in Fig. 6 may be due to resistance of ES-DC to killing by CTL that is attributed partly to the high level of expression of SPI-6, the granzyme B-specific protease inhibitor, in ES-DC (34). In addition, in the experiments shown in Fig. 6, we cultured spleen cells isolated from immunized mice for 5 days in the presence of RSV-M2 peptide to amplify RSV-specific CTL before the cytotoxicity assay, because we could not detect RSV-specific CTL activity in a direct ex vivo killing assay. Probably, in the data shown in Fig. 6, difference in the CTL activity induced in vivo by the different genotype of ES-DC may have been masked by this culture procedure.

In the present study, the MHC class II haplotype of ES-DC was always b while that of the recipient mice (BALB/c) was d. Therefore, there was mismatch in MHC class II haplotype between ES-DC and the recipient mice in all of the experiments. Because the mismatch of the MHC class II allele has been reported to not cause any acute elimination of transferred APC (24), the class II mismatch may not have negatively affected the priming of Ag-specific CTL in the present study. Instead, alloreactive helper T cells are expected to enhance the CTL response via cytokine production, although we did not experimentally address this issue in the present study.

Theoretically, the issue of histocompatibility related to the ES cell-based medical technology may be resolved by the recent development of induced pluripotent stem (iPS) cells that can be generated by introduction of several defined genes into somatic cells (35–38). However, the medical application of iPS cells nevertheless has some drawbacks. The use of virus vectors is necessary to generate iPS cells and generation of iPS cells for individual patients may be too costly, time consuming, and labor-intensive to be broadly applied. The genetic modification of ES cells or iPS cells to modify cell surface HLA class I by the presently reported methods may be more economical, faster and thus, more realistic than the individual generation of "fully personalized iPS cells".

Although targeted gene disruption of OCT4 and HPRT in human ES cells has been reported (39), the methodology of gene targeting for human ES cells has not been well established at present. Therefore, as an alternative strategy, we are planning to generate iPS cells from patients with Type I bare lymphocyte syndrome caused by mutation of the TAP 1 or TAP 2 gene (40, 41). Once a clone of TAP- or β_2m-deficient human ES or iPS cells is established, a premade library of pluripotent stem cell clones expressing various types of HLA class I can be generated by the introduction of various HLA class I genes. Such a pluripotent stem cell bank may serve as a source of not only DC but also of various kinds of differentiated cells that may be useful in the field of regenerative medicine.

Disclosures

The authors have no financial conflict of interest.

References

1. Banchereau, J., and A. Palucka. 2005. Dendritic cells as therapeutic vaccines against cancer. *Nat. Rev. Immunol.* 5: 296–306.
2. Brossart, P., S. Wirths, G. Stuhler, V. Reichardt, L. Kanz, and W. Brugger. 2000. Induction of cytotoxic T-lymphocyte responses in vivo after vaccinations with peptide-pulsed dendritic cells. *Blood* 96: 3102–3108.
3. Banchereau, J., and R. Steinman. 1998. Dendritic cells and the control of immunity. *Nature* 392: 245–252.
4. Fairchild, P., F. Brook, R. Gardner, L. Graça, V. Strong, Y. Tone, M. Tone, K. Nolan, and H. Waldmann. 2000. Directed differentiation of dendritic cells from mouse embryonic stem cells. *Curr. Biol.* 10: 1515–1518.
5. Senju, S., S. Hirata, H. Matsuyoshi, M. Masuda, Y. Uemura, K. Araki, K. Yamamura, and Y. Nishimura. 2003. Generation and genetic modification of dendritic cells derived from mouse embryonic stem cells. *Blood* 101: 3501–3508.
6. Zhan, X., G. Dravid, Z. Ye, H. Hammond, M. Shamblott, J. Gearhart, and L. Cheng. 2004. Functional antigen-presenting leucocytes derived from human embryonic stem cells in vitro. *Lancet* 364: 163–171.

7. Slukvin, I., M. Vodyanik, J. Thomson, M. Gumenyuk, and K. Choi. 2006. Directed differentiation of human embryonic stem cells into functional dendritic cells through the myeloid pathway. *J. Immunol.* 176: 2924–2932.
8. Senju, S., H. Suemori, H. Zembutsu, Y. Uemura, S. Hirata, D. Fukuma, H. Matsuyoshi, M. Shimomura, M. Haruta, S. Fukushima, et al. 2007. Genetically manipulated human embryonic stem cell-derived dendritic cells with immune regulatory function. *Stem Cells* 25: 2720–2729.
9. Hirata, S., S. Senju, H. Matsuyoshi, D. Fukuma, Y. Uemura, and Y. Nishimura. 2005. Prevention of experimental autoimmune encephalomyelitis by transfer of embryonic stem cell-derived dendritic cells expressing myelin oligodendrocyte glycoprotein peptide along with TRAIL or programmed death-1 ligand. *J. Immunol.* 174: 1888–1897.
10. Motomura, Y., S. Senju, T. Nakatsura, H. Matsuyoshi, S. Hirata, M. Monji, H. Komori, D. Fukuma, H. Baba, and Y. Nishimura. 2006. Embryonic stem cell-derived dendritic cells expressing glypican-3, a recently identified oncofetal antigen, induce protective immunity against highly metastatic mouse melanoma, B16–F10. *Cancer Res.* 66: 2414–2422.
11. Matsuyoshi, H., S. Hirata, Y. Yoshitake, Y. Motomura, D. Fukuma, A. Kurisaki, T. Nakatsura, Y. Nishimura, and S. Senju. 2005. Therapeutic effect of α-galactosylceramide-loaded dendritic cells genetically engineered to express SLC/CCL21 along with tumor antigen against peritoneally disseminated tumor cells. *Cancer Sci.* 96: 889–896.
12. Bradley, J., E. Bolton, and R. Pedersen. 2002. Stem cell medicine encounters the immune system. *Nat. Rev. Immunol.* 2: 859–871.
13. Robertson, N., F. Brook, R. Gardner, S. Cobbold, H. Waldmann, and P. Fairchild. 2007. Embryonic stem cell-derived tissues are immunogenic but their inherent immune privilege promotes the induction of tolerance. *Proc. Natl. Acad. Sci. USA* 104: 20920–20925.
14. Kulkarni, A., H. R. Morse, J. Bennink, J. Yewdell, and B. Murphy. 1993. Immunization of mice with vaccinia virus-M2 recombinant induces epitope-specific and cross-reactive Kd-restricted $CD8^+$ cytotoxic T cells. *J. Virol.* 67: 4086–4092.
15. Doe, B., M. Selby, S. Barnett, J. Baenziger, and C. Walker. 1996. Induction of cytotoxic T lymphocytes by intramuscular immunization with plasmid DNA is facilitated by bone marrow-derived cells. *Proc. Natl. Acad. Sci. USA* 93: 8578–8583.
16. Zijlstra, M., E. Li, F. Sajjadi, S. Subramani, and R. Jaenisch. 1989. Germ-line transmission of a disrupted β 2-microglobulin gene produced by homologous recombination in embryonic stem cells. *Nature* 342: 435–438.
17. Senju, S., K. Iyama, H. Kudo, S. Aizawa, and Y. Nishimura. 2000. Immunocytochemical analyses and targeted gene disruption of GTPBP1. *Mol. Cell. Biol.* 20: 6195–6200.
18. Mortensen, R. M., D. A. Conner, S. Chao, A. A. Geisterfer-Lowrance, and J. G. Seidman. 1992. Production of homozygous mutant ES cells with a single targeting construct. *Mol. Cell. Biol.* 12: 2391–2395.
19. Joyce, S., I. Negishi, A. Boesteanu, A. D. DeSilva, P. Sharma, M. J. Chorney, D. Y. Loh, and L. Van Kaer. 1996. Expansion of natural ($NK1^+$) T cells that express α β T cell receptors in transporters associated with antigen presentation-1 null and thymus leukemia antigen positive mice. *J. Exp. Med.* 184: 1579–1584.
20. Hirata, S., H. Matsuyoshi, D. Fukuma, A. Kurisaki, Y. Uemura, Y. Nishimura, and S. Senju. 2007. Involvement of regulatory T cells in the experimental autoimmune encephalomyelitis-preventive effect of dendritic cells expressing myelin oligodendrocyte glycoprotein plus TRAIL. *J. Immunol.* 178: 918–925.
21. Raulet, D., P. Gottlieb, and M. Bevan. 1980. Fractionation of lymphocyte populations with monoclonal antibodies specific for LYT-2.2 and LYT-3.1. *J. Immunol.* 125: 1136–1143.
22. Ritchie, D. S., I. F. Hermans, J. M. Lumsden, C. B. Scanga, J. M. Roberts, J. Yang, R. A. Kemp, and F. Ronchese. 2000. Dendritic cell elimination as an assay of cytotoxic T lymphocyte activity in vivo. *J. Immunol. Methods* 246: 109–117.
23. Wells, J. W., C. J. Cowled, D. Darling, B. A. Guinn, F. Farzaneh, A. Noble, and J. Galea-Lauri. 2007. Semi-allogeneic dendritic cells can induce antigen-specific T-cell activation, which is not enhanced by concurrent alloreactivity. *Cancer Immunol. Immunother.* 56: 1861–1873.
24. Loyer, V., P. Fontaine, S. Pion, F. Hetu, D. C. Roy, and C. Perreault. 1999. The in vivo fate of APCs displaying minor H antigen and/or MHC differences is regulated by CTLs specific for immunodominant class I-associated epitopes. *J. Immunol.* 163: 6462–6467.
25. Hermans, I. F., D. S. Ritchie, J. Yang, J. M. Roberts, and F. Ronchese. 2000. $CD8^+$ T cell-dependent elimination of dendritic cells in vivo limits the induction of antitumor immunity. *J. Immunol.* 164: 3095–3101.
26. Hyoudou, K., M. Nishikawa, Y. Kobayashi, Y. Kuramoto, F. Yamashita, and M. Hashida. 2006. Inhibition of adhesion and proliferation of peritoneally disseminated tumor cells by pegylated catalase. *Clin. Exp. Metastasis* 23: 269–278.
27. Chang, A., B. Redman, J. Whitfield, B. Nickoloff, T. Braun, P. Lee, J. Geiger, and J. Mulé. 2002. A phase I trial of tumor lysate-pulsed dendritic cells in the treatment of advanced cancer. *Clin. Cancer Res.* 8: 1021–1032.
28. Wierecky, J., M. Mueller, and P. Brossart. 2006. Dendritic cell-based cancer immunotherapy targeting MUC-1. *Cancer Immunol. Immunother.* 55: 63–67.
29. Olsen, A., D. Stachura, and M. Weiss. 2006. Designer blood: creating hematopoietic lineages from embryonic stem cells. *Blood* 107: 1265–1275.
30. Laffont, S., J. Coudert, L. Garidou, L. Delpy, A. Wiedemann, C. Demur, C. Coureau, and J. Guéry. 2006. $CD8^+$ T-cell-mediated killing of donor dendritic cells prevents alloreactive T helper type-2 responses in vivo. *Blood* 108: 2257–2264.
31. Van Kaer, L., P. Ashton-Rickardt, H. Ploegh, and S. Tonegawa. 1992. TAP1 mutant mice are deficient in antigen presentation, surface class I molecules, and $CD4^-8^+$ T cells. *Cell* 71: 1205–1214.
32. Zijlstra, M., M. Bix, N. Simister, J. Loring, D. Raulet, and R. Jaenisch. 1990. β2-microglobulin deficient mice lack $CD4^-8^+$ cytolytic T cells. *Nature* 344: 742–746.
33. Yang, J., S. Huck, R. McHugh, I. Hermans, and F. Ronchese. 2006. Perforin-dependent elimination of dendritic cells regulates the expansion of antigen-specific $CD8^+$ T cells in vivo. *Proc. Natl. Acad. Sci. USA* 103: 147–152.
34. Fukuma, D., H. Matsuyoshi, S. Hirata, A. Kurisaki, Y. Motomura, Y. Yoshitake, M. Shinohara, Y. Nishimura, and S. Senju. 2005. Cancer prevention with semi-allogeneic ES cell-derived dendritic cells. *Biochem. Biophys. Res. Commun.* 335: 5–13.
35. Takahashi, K., and S. Yamanaka. 2006. Induction of pluripotent stem cells from mouse embryonic and adult fibroblast cultures by defined factors. *Cell* 126: 663–676.
36. Takahashi, K., K. Tanabe, M. Ohnuki, M. Narita, T. Ichisaka, K. Tomoda, and S. Yamanaka. 2007. Induction of pluripotent stem cells from adult human fibroblasts by defined factors. *Cell* 131: 861–872.
37. Yu, J., M. Vodyanik, K. Smuga-Otto, J. Antosiewicz-Bourget, J. Frane, S. Tian, J. Nie, G. Jonsdottir, V. Ruotti, R. Stewart, et al. 2007. Induced pluripotent stem cell lines derived from human somatic cells. *Science* 318: 1917–1920.
38. Lowry, W., L. Richter, R. Yachechko, A. Pyle, J. Tchieu, R. Sridharan, A. Clark, and K. Plath. 2008. Generation of human induced pluripotent stem cells from dermal fibroblasts. *Proc. Natl. Acad. Sci. USA* 105: 2883–2888.
39. Zwaka, T., and J. Thomson. 2003. Homologous recombination in human embryonic stem cells. *Nat. Biotechnol.* 21: 319–321.
40. de la Salle, H., D. Hanau, D. Fricker, A. Urlacher, A. Kelly, J. Salamero, S. Powis, L. Donato, H. Bausinger, and M. Laforet. 1994. Homozygous human TAP peptide transporter mutation in HLA class I deficiency. *Science* 265: 237–241.
41. Furukawa, H., S. Murata, T. Yabe, N. Shimbara, N. Keicho, K. Kashiwase, K. Watanabe, Y. Ishikawa, T. Akaza, K. Tadokoro, et al. 1999. Splice acceptor site mutation of the transporter associated with antigen processing-1 gene in human bare lymphocyte syndrome. *J. Clin. Invest.* 103: 755–758.

European Journal of Immunology Molecular immunology

B-Raf-mediated signaling pathway regulates T cell development

Hirotake Tsukamoto[*1], *Atsushi Irie*[1], *Satoru Senju*[1], *Antonis K. Hatzopoulos*[2,3], *Leszek Wojnowski*[4] *and Yasuharu Nishimura*[1]

[1] Department of Immunogenetics, Graduate School of Medical Sciences, Kumamoto University, Kumamoto, Japan
[2] Department of Medicine and Cell & Developmental Biology, Division of Cardiovascular Medicine, Vanderbilt University Medical Center, Nashville, TN, USA
[3] Institute for Clinical Molecular Biology and Tumor Genetics, GSF-Research Center for Environment and Health, Munich, Germany
[4] Department of Pharmacology, Johannes Gutenberg University, Mainz, Germany

The activities of the Raf kinase family proteins control extracellular signal-regulated kinase (ERK) activation in many aspects of cellular responses. However, the relative contributions of individual isozymes to cellular functions including T cell responses are still unclear. In addition to Raf-1, another Raf family kinase, B-Raf, is expressed in murine thymocytes and peripheral T cells, and its activation was induced by TCR stimulation. Here, we investigated the function of B-Raf in development of T cells by generating chimeric mice in which a T cell-compromised host was reconstituted with fetal liver-derived cells from embryonic lethal B-Raf-deficient mice. Although B-Raf was dispensable for normal T cell lineage differentiation at the $CD4^-CD8^-$ double-negative stage, thymocytes in the chimeric mice derived from $B\text{-}Raf^{-/-}$ cells exhibited a drastic arrest of differentiation at the $CD4^+CD8^+$ double-positive stage, suggesting that B-Raf is crucial for T cell development, especially for the transition to $CD4^+$ and $CD8^+$ single-positive thymocytes. Regarding intracellular signaling, we found that activation of ERK following TCR stimulation was impaired in the thymocytes from the chimeric mice. In conclusion, we present first evidence for the important role of B-Raf-mediated signaling in T cell development.

Received 29/4/07
Revised 24/10/07
Accepted 10/12/07

[DOI 10.1002/eji.200737430]

Key words: B-Raf · Cell differentiation · T cells · T cell receptors

Supporting Information for this article is available at http://www.wiley-vch.de/contents/jc_2040/2008/37430_s.pdf

Introduction

In thymus, thymocyte development is responsible for generation of mature T cells. Developing thymocytes can be classified into three stages of increasing maturity, $CD4^-CD8^-$ double-negative (DN), $CD4^+CD8^+$ double-positive (DP) and $CD4^+$ or $CD8^+$ single-positive (SP) subsets [1, 2]. TCR signaling mediates these processes, especially positive and negative selection at the DP stage. A favored hypothesis, the avidity model, postulates that positively selecting peptide/MHC complexes interact with TCR with low avidity, delivering a weak signal that rescues cells from their default fate (death by neglect) without inducing apoptotic cell death of

Correspondence: Yasuharu Nishimura, Department of Immunogenetics, Graduate School of Medical Sciences, Kumamoto University, Honjo 1-1-1, Kumamoto 860–8556, Japan
Fax: +81-96-373-5314
e-mail: mxnishim@gpo.kumamoto-u.ac.jp

Abbreviations: DN: double negative · **DP:** double positive · **FL:** fetal liver · **OP9-DL1:** OP9 cells expressing delta-like1 · **SP:** single positive

* Current address: Trudeau Institute, 154 Algonquin Avenue, Saranac Lake, NY 12983

thymocytes [2, 3]. On the other hand, negatively selecting peptide/MHC complexes interact with TCR with high avidity, delivering an intense signal, which induces apoptosis [2, 3].

A number of studies have revealed that the MAPK pathway consisting of p21Ras, Raf, MEK and ERK represents one of the important signaling cascades coupled to TCR-mediated responses, including the determination of cell fate at various stages of thymic selection [4, 5]. Transgenic expression of dominant-negative or constitutively active forms of Ras, Raf or MEK1 all revealed that the MAPK pathway is implicated in positive selection at the $CD4^+CD8^+$ DP stage [6–9]. Consistent with these reports, ERK activation is involved in the most critical events during TCR signaling and plays a crucial role in positive selection [4, 5]. In addition to positive selection, ERK activation is also known to be indispensable for the intracellular signals promoting the first β-selection checkpoint [10] and lineage commitment of mature $CD4^+$ or $CD8^+$ SP cells [11]. Therefore, understanding how TCR signaling in thymocytes results in ERK activation is important for elucidation of the mechanisms of thymocyte development.

A-Raf, B-Raf and C-Raf (also called Raf-1) constitute a Raf kinase family that contributes to activation of the MEK/ERK pathway in various aspects of proliferation, differentiation and apoptosis in mammalian cells [12–15]. Although the individual Raf genes have some apparent functional redundancies with each other in ERK regulation, the different phenotypes of each Raf kinase-deficient mouse suggest that they have specific and non-redundant functions [12, 16–19], which seem to be due to their distinct expression patterns [20] and differences in the thresholds for activation [15, 21, 22].

In T cells, Raf-1 is thought to regulate TCR-mediated activation [23], whereas the expression and function of B-Raf remain controversial. Previously we reported that B-Raf activation is regulated by Ras and mediates sustained ERK activation and subsequent IL-2 production upon TCR stimulation in human T cells [22, 24]. In addition, enforced expression of B-Raf in mouse $CD4^+$ T cells resulted in augmentation of their proliferation and prevention of anergy induction [25]. Reciprocally, it was demonstrated that superantigen-induced anergic T cells down-regulate the expression of B-Raf *in vivo* [26]. Taken together, current data in T cells indicate that B-Raf may be an important signaling molecule in TCR-mediated responses.

Although B-Raf-deficient T cells would be a powerful tool for analyses of B-Raf function, T cells cannot be obtained from B-Raf-null mice, since targeted disruption of the murine B-Raf gene results in embryonic lethality caused by defects of vasculargenesis during mid-gestation [19]. Therefore, the *in vivo* role of B-Raf on development and activation of T cells remains to be elucidated. To overcome the early embryonic lethality of $B\text{-}Raf^{-/-}$ mice, we generated chimeric $RAG2^{-/-}$ mice in which T cells were reconstituted using hematopoietic stem cells (HSC) or T cell precursor cells derived from fetal liver (FL) cells in $B\text{-}Raf^{-/-}$ mice and examined the role of B-Raf in T cell development. These approaches demonstrated that B-Raf is a positive regulator of T cell development. Furthermore, we found that B-Raf contributes to the promotion of TCR-mediated ERK activation at the DP stage. Our data provide evidence that B-Raf plays a specific and crucial role in T cell development *in vivo*.

Results

Expression and activation of B-Raf in thymocytes

To examine B-Raf expression, DN-arrested thymocytes from $RAG2^{-/-}$ mice [27], purified $CD4^+CD8^+$ DP thymocytes and peripheral T cells from wild-type C57BL/6 mice were immunoblotted with anti-B-Raf Ab (Fig. 1A). Substantial expression of B-Raf protein could be detected in all subsets of immature thymocytes and peripheral T cells. In addition, it was shown that T cells isolated from $B\text{-}Raf^{+/-}$ mice express less B-Raf protein than T cells from wild-type mice. $B\text{-}Raf^{-/-}$ T cells isolated from $RAG2^{-/-}$ chimeric mice that had been reconstituted with B-Raf-deficient HSC (see section *Requirement of B-Raf for the development of single-positive thymocytes*) did not exhibit B-Raf expression but did express Raf-1 and ERK. No compensatory increase in Raf-1 expression was observed in B-Raf-deficient T cells. B-Raf protein was highly expressed in PC12 cells and B-Raf-transfected Jurkat cells, which were utilized as positive controls [24, 28].

Next we examined whether B-Raf activity is regulated by TCR stimulation. In thymocytes, TCR stimulation induced up-regulation of the kinase activity of B-Raf. MEK phosphorylation was confirmed using Ab specific for phosphorylated MEK (data not shown). This activation was prolonged for up to 60 min and was coincident with ERK activation (Fig. 1B, C). As expected, PMA stimulation also induced B-Raf activation (Fig. 1B). However, surprisingly, Raf-1 activation was not detected up to 60 min after TCR stimulation, although substantial ERK activation was observed under the same stimulatory conditions (Fig. 1C), while Raf-1 activation could be observed in PMA-stimulated thymocytes (Fig. 1B). In TCR-stimulated peripheral T cells, activation of both Raf-1 and B-Raf was induced (Fig. 1D). These results could be attributed to the lower activation threshold of B-Raf than Raf-1 in response to TCR

stimulation [22]. The findings of TCR stimulation-inducible B-Raf activation prompted us to hypothesize that B-Raf could play a role in TCR-mediated T cell responses in thymocytes.

β-selection proceeds normally *in vitro* and *in vivo* in B-Raf-deficient T cell progenitors

T cell progenitors enter the thymus as $CD44^+CD25^-$ cells and soon acquire expression of CD25. The next transition, from $CD44^-CD25^+$ (DN3 stage) to $CD44^-CD25^-$ (DN4 stage), is termed β-selection; this step requires pre-TCR-mediated signals and is coincident with extensive proliferation [29]. These developmental events of T cell progenitors at the DN stage are mimicked in an *in vitro* co-culture system using OP9 cells expressing delta-like1 (OP9-DL1) [30, 31]. Using this system, we assessed the requirement for B-Raf during developmental progression of the DN subpopulation and in β-selection.

Given that by embryonic day 11–12, definitive hematopoietic progenitor cells capable of generating T, B and myeloid cells colonize the FL [32], we utilized FL cells from B-$Raf^{-/-}$ fetuses prior to embryonic death (embryonic day 11.5–12.5) as a source of B-Raf-deficient HSC. As shown in Fig. 2A, kinetic analysis of differentiation from the FL cells co-cultured with OP9-DL1 demonstrated that both B-$Raf^{+/+}$ and B-$Raf^{-/-}$ DN cells acquire DN3–4 phenotypes with loss of CD44 expression at day 8 of the co-culture. At this time point, there were comparably low frequencies of $NK1.1^+$ cells (<3%) and $B220^+$ cells (<0.5%) in B-$Raf^{+/+}$ and B-$Raf^{-/-}$ FL cell cultures (data not shown). Moreover, at day 15 of co-culture, regardless of the

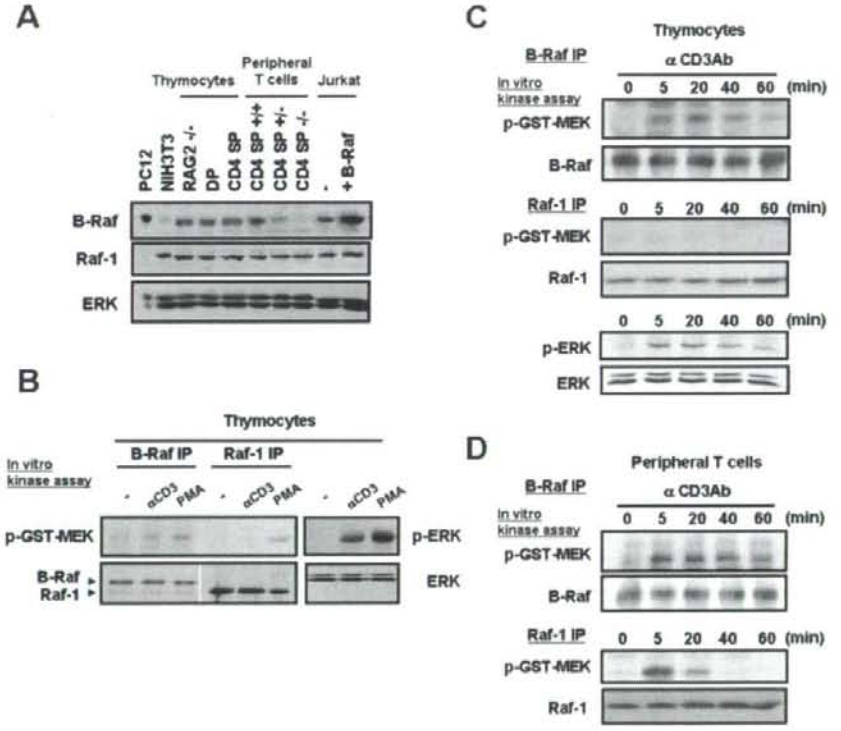

Figure 1. Expression and TCR-mediated activation of B-Raf in T cells. (A) Western blotting analysis of B-Raf expression in thymocytes from $RAG2^{-/-}$ mice, DP and SP thymocytes sorted from C57BL/6 mice, peripheral (splenic) T cells from $RAG2^{-/-}$ chimeras reconstituted with B-$Raf^{+/+}$, B-$Raf^{+/-}$ or B-$Raf^{-/-}$ FL cells, as well as mock- and B-Raf-transfected Jurkat cells. Raf-1 and ERK blottings are shown as loading controls. PC12 and NIH3T3 were utilized as positive and negative controls of B-Raf expression, respectively. (B, C) *In vitro* kinase assays for Raf-1 and B-Raf isolated from thymocytes stimulated with 10 μg/mL anti-CD3 Ab or 25 ng/mL PMA for 10 min (B) or anti-CD3Ab for the indicated times (C). Recombinant GST-MEK was used as a substrate, and incorporated ^{32}P radioactivity was visualized by autoradiography (upper left panel). ERK phosphorylation was determined by blotting with an antibody specific for phosphorylated ERK. Equal loading of each Raf isoform and ERK was confirmed (lower left panels). (D) Splenic T cells were stimulated with 5 μg/mL anti-CD3 Ab for the indicated times in an *in vitro* kinase assay for B-Raf and Raf-1 performed as described in (B).

B-Raf status of the T cell progenitors, $CD4^+CD8^+$ DP cells were efficiently induced (Fig. 2A, lower panels). The number of harvested B-$Raf^{-/-}$ Thy-1^+ cells decreased as compared with B-$Raf^{+/+}$ cells, which might be the consequence of a lower precursor frequency in B-$Raf^{-/-}$ FL cells rather than differentiation defects of B-$Raf^{-/-}$ DN cells ([16] and Supporting Information Fig. 1).

Because cellular expansion is one of the hallmarks of β-selection [29, 33], we examined the requirement of B-Raf for this event. For this purpose, cells harvested at day 8 of OP9-DL1 co-culture ($CD25^+$ DN2–3 stage) were labeled with a mitotic tracker, CFSE, and reseeded onto OP9-DL1. OP9 cells expressing GFP (OP9-GFP) were utilized as a mock-transfected control of OP9-DL1 [31]. As shown in Fig. 2B, the degree of dilution of CFSE revealed that B-Raf deficiency was permissive for pre-TCR-mediated proliferation during the transition from $CD25^+$ DN3 to $CD25^-$ DN4 stage in a delta-like1-dependent manner.

To determine the dependency of *in vivo* development of the T cell lineage on B-Raf, we generated chimeric mice by transferring HSC from FL of B-$Raf^{-/-}$ fetuses into T cell-compromised $RAG2^{-/-}$ mice. In support of the results obtained from the *in vitro* culture system of DN cell differentiation, B-Raf-deficient thymocytes underwent normal phenotypic progression to DN4 stage, as did B-$Raf^{+/+}$ thymocytes reconstituted in the FL chimeric mice (Fig. 2C). Taken together, these results suggest that B-Raf is not necessary for T cell development at the DN stages and pre-TCR-mediated β-selection both *in vitro* and *in vivo*.

Requirement of B-Raf for the development of single-positive thymocytes

To address whether B-Raf is required for further T cell development, we first examined the CD4 and CD8 expression profiles of B-$Raf^{+/+}$ and B-$Raf^{-/-}$ thymocytes in FL chimeras. Surprisingly, we found that B-$Raf^{-/-}$ FL

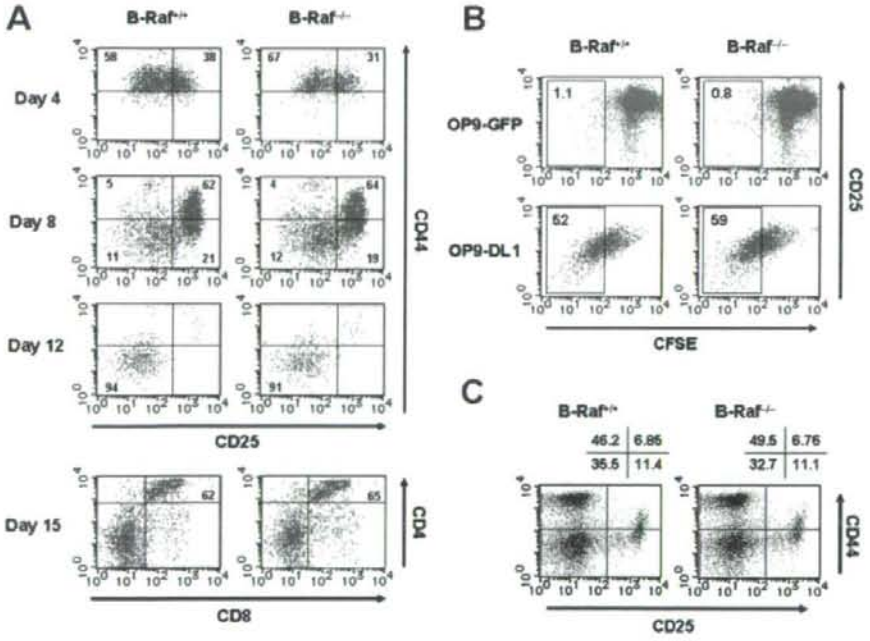

Figure 2. Pre-TCR-mediated β-selection is not affected by B-Raf deficiency. (A) Phenotypic changes of DN cells differentiated from wild-type and B-$Raf^{-/-}$ FL-derived progenitors in co-culture with OP9-DL1 for various times. Developmental progression of the T cell lineage was assessed on days 4, 8 and 12 by CD25 and CD44 expression profiles on $CD4^-CD8^-$ DN-gated cells. In the lowest panels, percentages of $CD4^+CD8^+$ DP cells co-cultured with OP9-DL1 for 15 days are indicated. Lymphoid cells were gated based on their SSC and FSC profiles. (B) DN T cell progenitors derived from B-$Raf^{+/+}$ and B-$Raf^{-/-}$ FL cells co-cultured with OP9-DL1 for 8 days were loaded with CFSE and re-seeded on OP9 GFP (upper panels) or OP9 DL1 (lower panels). After 48 h, proliferation indicated by CFSE dilution and CD25 expression on DN cells during β-selection were determined. Dot plots show cells gated to eliminate $CD4^+CD8^+$ DP and OP9-DL1 cells. (C) Thymocytes from B-$Raf^{+/+}$ and B-$Raf^{-/-}$ chimeric mice 7 wk after transfer of FL cells into $RAG2^{-/-}$ mice were isolated by positively sorting with anti-Thy-1 magnetic beads. The plots for CD44 and CD25 expression were gated on the $CD4^-CD8^-$ DN population. The data are representative of three animals per group in two independent experiments with similar results, and the percentages of gated cells that fall into each quadrant are shown.

chimeras showed accumulation of $CD4^+CD8^+$ DP cells, and both $CD4^+$ SP and $CD8^+$ SP thymocytes derived from B-$Raf^{-/-}$ cells were markedly decreased as compared with B-$Raf^{+/+}$ controls (Fig. 3A, upper panels). On the other hand, detectable Thy-1^+ T cells and $B220^+$ B cells were reconstituted to similar levels in spleen in both chimeric mice (Fig. 3A, lower panels). Despite the lower thymic output of T cells in B-$Raf^{-/-}$ FL chimeras, accumulation of T cells in the periphery was observed at a similar proportion as in control mice; this seemed to be due to lymphopenia-induced proliferation of a small number of B-$Raf^{-/-}$ T cells to complement the limited T cell niche, leading to accumulation in the periphery [34]. In fact, compared to control mice, B-$Raf^{-/-}$ chimeric mice exhibited an increased $CD44^{hi}$ population, which is reminiscent of T cells undergoing lymphopenia-induced proliferation (Fig. 3B).

Thymic cellularity of B-$Raf^{-/-}$ chimeras was typically about half of that of B-$Raf^{+/+}$ mice, and the absolute numbers of $CD4^-CD8^-$ DN and $CD4^+CD8^+$ DP B-$Raf^{-/-}$ cells were slightly decreased as compared with control mice (Fig. 3C). Furthermore, significantly reduced numbers of $CD4^+$ SP and $CD8^+$ SP cells were observed in B-$Raf^{-/-}$ thymocytes. These results raised the possibility that B-Raf is required for further development of thymocytes after β-selection.

The results from such FL chimeras generated by reconstitution with HSC have to be interpreted with caution, especially with regard to the possibility of extrinsic effects of non-T cell lineages and of the difference in the frequency of HSC giving lymphoid subsets between mutant and wild-type FL cells [32]. To confirm the T cell autonomous effects of B-Raf deficiency on thymocyte development at the DP stage, we reconstituted $RAG2^{-/-}$ mice with the B-$Raf^{-/-}$ T cell lineage from committed T progenitor cells at DN2–3 stage generated by 8 days co-culture with OP9-DL1 (Fig. 2). Recapitulating the results from FL chimeras, when $RAG2^{-/-}$ mice were reconstituted with DN cells, the majority of B-$Raf^{-/-}$ thymocytes were retained in the $CD4^+CD8^+$ DP stage (B-$Raf^{+/+}$, 69% *versus* B-$Raf^{-/-}$, 82%), and $CD4^+$ or $CD8^+$ SP populations were decreased (Fig. 4A, upper panels). Moreover, significant decreases in SP cell numbers were observed in the B-$Raf^{-/-}$ chimeras (Supporting Information Fig. 2A). In the periphery, the two chimeric mice possessed comparable $CD4^+$ SP and $CD8^+$ SP frequencies and numbers (Fig. 4A, lower panels and Supporting Information Fig. 2B). As expected and in contrast to FL chimeras, we observed transient but not long-term repopulation of DP thymocytes derived from transferred DN cells in B-$Raf^{+/+}$ chimeras (measured 4 wk after transfer), whereas B-$Raf^{-/-}$ cells remained in the DP stage up to 6 wk after transfer (data not shown).

After DP cells undergo positive selection, the expression of TCR increases, and thus TCR^+ DP and $CD4^+$ or $CD8^+$ SP cells are expected to be positively selected [3, 7, 8]. We therefore examined the TCR expression on B-Raf $^{+/+}$ and B-$Raf^{-/-}$ thymocytes. As

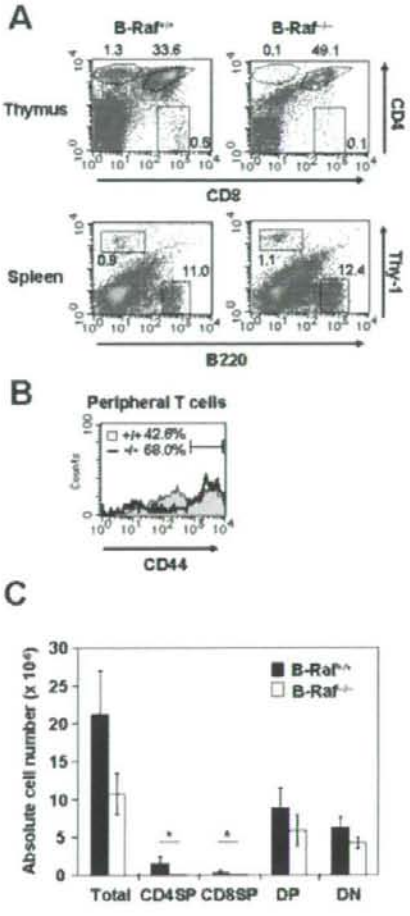

Figure 3. Inefficient production of $CD4^+$ and $CD8^+$ SP cells in B-Raf-deficient thymocytes. (A) Single-cell suspensions of thymocytes (upper panels) and spleen cells (lower panels) were isolated from age-matched B-$Raf^{+/+}$ and B-$Raf^{-/-}$ FL chimeric mice 8 wk after transfer, stained with Ab against CD4, CD8, B220 and TCR-β chain, and analyzed by flow cytometry. Lymphoid cells were gated based on SSC and FSC. The percentages of total thymocytes and spleen cells that fall into each region are indicated. (B) Cell surface expression of CD44 on peripheral T cells isolated from spleen and lymph nodes of B-Raf $^{+/+}$ (filled gray) and B-$Raf^{-/-}$ (bold line) FL chimeric mice. (C) Thymi were harvested 8–12 wk after transfer and the cell suspension enumerated. After calculating the percentage of lymphoid cells (~85% of total) on the basis of FSC/SSC, the numbers of the indicated population were calculated (mean ± SD). Data are based on four to five samples of thymus (*$p<0.01$). All data are representative of at least three B-Raf $^{+/+}$ and B-$Raf^{-/-}$ chimeric mice in two independent experiments.

shown in Fig. 4B, B-Raf$^{-/-}$ TCR^{hi} thymocytes were reduced by approximately 40%, with a concomitant decrease in mature CD4$^+$ or CD8$^+$ SP TCR^{hi} thymocytes in B-Raf$^{-/-}$ chimeras.

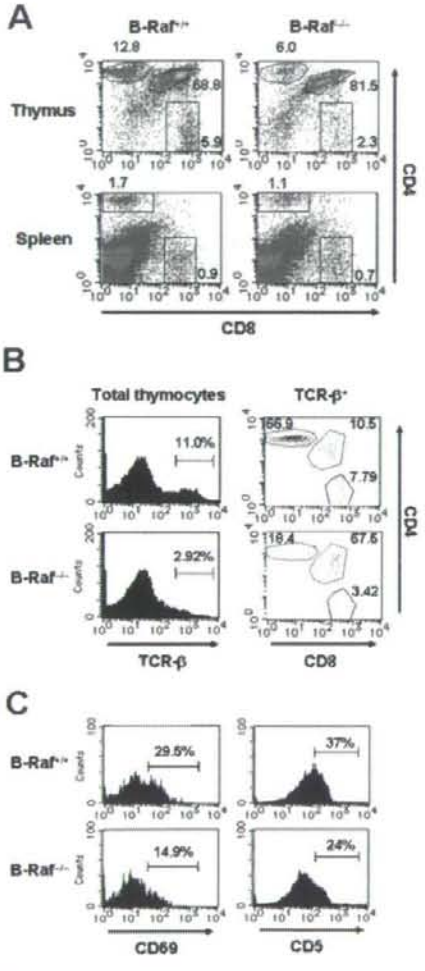

Figure 4. Attenuated thymocyte development in B-Raf$^{-/-}$ chimeric mice. (A) CD4 and CD8 staining on total thymocytes (upper panels) and spleen cells (lower panels) from chimeric mice 4 wk after transfer of B-Raf$^{+/+}$ or B-Raf$^{-/-}$ DN cells generated by co-culture with OP9-DL1. The cells were analyzed by flow cytometry. The percentages of cells in each population are indicated within each dot plot. (B) Representative histograms of TCR-β chain expression on total thymocytes (left panels) and dot plots of CD4 and CD8 staining on cells that express high levels of TCR (right panels). (C) Representative histograms of CD69 (left panels) and CD5 (right panels) expression on thymocytes gated on CD4$^+$CD8$^+$ DP cells from the B-Raf$^{+/+}$ and B-Raf$^{-/-}$ chimeric mice described in (A). All data are representative of at least three independent experiments.

We next hypothesized that the failure of DP cells to efficiently undergo further differentiation in the absence of B-Raf could be due to a defect in the responsiveness of the DP cells to TCR signaling. We investigated this hypothesis by staining for CD69 and CD5 on B-Raf$^{+/+}$ and B-Raf$^{-/-}$ thymocytes, because up-regulation of these two markers on thymocytes is dependent on productive TCR signaling, and DP thymocytes that have undergone positive selection can be enumerated by measuring the relative expression levels of CD69 and CD5 [3, 35, 36]. As shown in Fig. 4C and Table 1, wild-type DP cells exhibited higher frequencies of CD69$^+$ and CD5$^+$ cells than their B-Raf$^{-/-}$ counterparts. These results suggested that the abnormal phenotype of B-Raf$^{-/-}$ thymocytes is T cell autonomous, and B-Raf$^{-/-}$ DP thymocytes do not transmit sufficient TCR signals to lead to thymocyte maturation, resulting in the DP arrest.

B-Raf is a positive regulator of ERK activation in thymocytes

Progress of thymocyte differentiation at the DP stage is critically dependent on TCR-mediated intracellular signaling [3]. To evaluate whether the inability of B-Raf-deficient thymocytes to differentiate into the SP stage is due to impaired signaling through the TCR, we measured the activation status of ERK following TCR stimulation, since it has been shown that ERK activity is regulated by TCR-mediated signaling and acts as an important regulator of thymic selection [4]. To determine the levels of ERK activation in thymocytes, we performed a flow cytometry-based analyses using a specific anti-phospho-ERK Ab. As shown in Fig. 5, TCR stimulation induced ERK activation in wild-type DP thymocytes, and the ERK activation was drastically attenuated in B-Raf$^{-/-}$ DP cells at 5 and 20 min after stimulation. As expected, TCR-mediated ERK activation in both wild-type and B-Raf$^{-/-}$ thymocytes was completely blocked by the treatment of cells with the MEK inhibitor U0216. In contrast to TCR stimulation, stimulation with PMA evoked comparable ERK activation in B-Raf$^{-/-}$ and B-Raf$^{+/+}$ thymocytes (Fig. 5). It was demonstrated that B-Raf deficiency specifically reduced TCR-mediated ERK activation in the DP thymocytes, while PMA stimulation bypassed B-Raf function and induced full ERK activation comparable to that of the TCR-stimulated B-Raf$^{+/+}$ DP thymocytes. Collectively, these results suggest that the developmental arrest of SP transition in B-Raf-deficient thymocytes reflects, at least in part, a defective cellular response to the TCR-mediated ERK activation pathway.

Table 1. Decreased frequency of mature thymocytes in B-Raf$^{-/-}$ chimeric mice.

Cell Subset	B-Raf$^{+/+}$ chimeras	B-Raf$^{-/-}$ chimeras[a)]	p values[b)]
TCR-β^{hi} (% in total)[c)]	9.58±1.6	3.40±1.3	<0.01
CD69$^+$ (% in DP)[c)]	26.9±3.0	15.9±2.6	<0.01
CD5$^+$ (% in DP)[c)]	36.2±3.5	25.9±4.7	<0.05

a) Thymi from control B-Raf$^{+/+}$ chimeras (n=4) or B-Raf$^{-/-}$ chimeras (n=4) were harvested 8–12 wk after transfer, and cells were stained with the indicated subset marker.

b) p values were calculated for frequencies using a two-tailed Student's t-test, which was considered significant at $p<0.05$.

c) Each value represents the frequency of the indicated population within total thymocytes or the CD4$^+$CD8$^+$ DP population. Mean percentages of the indicated populations are shown with SD.

Discussion

In this study, we provide convincing evidence for B-Raf expression in thymocytes and peripheral T cells. Furthermore, the analyses of T cells lacking B-Raf demonstrates an appreciable impact of B-Raf in thymocyte development.

It has previously been reported that B-Raf is not expressed in T cells and, therefore, might not play a role for T cells [25, 37]. This lack of observed B-Raf expression in T cells can be explained by a much lower expression level of B-Raf in human and murine T cells when compared with the robust expression of B-Raf in PC12 cells (Fig. 1 and [25]); there might be a relative difficulty to detect B-Raf expression in T cells under conditions in which comparable loading of total protein is done for T cells and PC12 cells. However, supporting our observations, several groups independently reported that B-Raf is expressed in human and murine T cells [24, 26, 38–40]. Based on our findings and these reports showing B-Raf expression, we have concluded that both murine thymocytes and peripheral T cells express B-Raf, which prompted us to investigate the function of B-Raf in T cells.

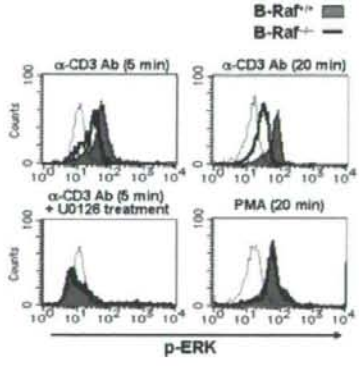

Figure 5. Total thymocytes were stimulated by crosslinking of CD3 with 10 μg/mL anti-CD3 Ab and anti-hamster Ig Ab for 5 or 20 min (upper panels) or by incubation with 25 ng/mL PMA for 20 min (lower right panel). Cells were treated for 30 min with 10 μM U0126 prior to TCR stimulation (lower left panel). Histograms show profiles of phospho-ERK in B-Raf$^{+/+}$ (filled gray) and B-Raf$^{-/-}$ (bold line) cells gated on CD4$^+$CD8$^+$ DP cells from DN cell-chimeric mice. Dotted lines indicate the status of phospho-ERK in unstimulated B-Raf$^{+/+}$ DP cells. The data are from one representative of three independent experiments.

The reconstitution of immunocompromised RAG2$^{-/-}$ hosts with B-Raf$^{-/-}$ HSC or T cell progenitors allowed us to dissect the contribution of B-Raf to thymocyte development and T cell activation. Thymocytes lacking B-Raf showed a profound increase in the DP fraction and a proportional decrease in both the SP fractions and TCR-β^+ mature thymocytes, suggesting an important role for B-Raf in T cells during late thymic development, particularly in the transition from DP thymocytes to the SP stage. Furthermore, ERK activation was impaired in B-Raf-deficient DP thymocytes (Fig. 4). These results support the notion that ERK is a critical molecule for efficient transition from the DP to SP stage [4, 5]. However, unlike ERK$^{-/-}$ thymocytes, the developmental progression from DN3 to DN4 stage (β-selection) was not attenuated in B-Raf$^{-/-}$ thymocytes (Fig. 2 and [4]). This raises the possibility that ERK activation is complemented by other up-stream molecules at this checkpoint. The most likely candidate is Raf-1, whose activation may overcome B-Raf deficiency during β-selection. Supporting this interpretation, it has been reported that active Raf-1 is sufficient to mediate β-selection even in the absence of pre-TCR signaling [41].

In contrast, the prominent phenotype in B-Raf$^{-/-}$ thymocytes at the DP stage seemed to be due to the inability of Raf-1 to compensate for B-Raf function. Indeed, Raf-1 activation did not coincide with ERK activation in TCR-stimulated thymocytes (Fig. 1 and [39]), and B-Raf was necessary for TCR-stimulated ERK activation in DP thymocytes (Fig. 4). The defect of ERK activation was not observed in B-Raf$^{-/-}$ thymocytes treated with PMA, which provoked substantial activation of the Raf-1-ERK pathway. It is interesting to note that thymocytes expressing dominant-interfering mutants of Raf and Ras also exhibited DP arrest [6–8]